	JAMILA European Commission TEMPUS	
Joint mAster of Mediterranean Initiatives on renewabLe and sustainAble energy		

Palestine Polytechnic University

Deanship of Graduate Studies and Scientific Research

Master Program of Renewable Energy and Sustainability

Assessment the Influence of Grid Connected Photovoltaic System on Medium Voltage Network in Tubas

---

By

Yehya Nadi Hassouneh

Supervisor

Prof Abdel-karim Daud

Thesis submitted in partial fulfillment of requirements of the degree

Master of Science in Renewable Energy & Sustainability

April, 2019

The undersigned hereby certify that they have read, examined and recommended to the Deanship of Graduate Studies and Scientific Research at Palestine Polytechnic University and the Faculty of Science at Al-Qdus University the approval of a thesis entitled:

Assessment the Influence of Grid Connected Photovoltaic System on Medium Voltage Network in Tubas

Submitted by

Yehya Nadi Hassouneh

In partial fulfillment of the requirements for the degree of Master in Renewable Energy & Sustainability.

Graduate Advisory Committee:

Prof. Abdel-Karim Daud
(Supervisor), Palestine Polytechnic University.

Signature: __________________ Date:____________

Prof. Sameer Hanna
(Internal committee member), Palestine Polytechnic University.

Signature: __________________ Date:____________

Prof. Marwan Mahmoud
(External committee member), An-Najah National University.

Signature: __________________ Date:____________

Thesis Approved by:

Name: Dr. Murad Abu Sbeih

Dean of Graduate Studies & Scientific Research

Palestine Polytechnic University

Signature:……………………………………

Date:……………………………………

Assessment the Influence of Grid Connected Photovoltaic System on Medium Voltage Network in Tubas

Submitted by

Yehya Nadi Hassouneh

ABSTRACT

The increasing of electrical energy consumption and the immediate need of electricity in Palestine, lead us to think about enhancing and developing the electrical power system. Using of renewable energy systems, especially solar energy is one of the solutions to produce sustainable and environmentally friendly electrical energy systems in Palestine due to its location with a high potential of solar radiation. There are three PV plants installed in three different locations in Tubas medium voltage network which are Maslamani plant and two Czechia plants with 3 MW and 470 kW respectively, the total power output from the PV systems could reach 16% of the feeder load. These power plants were installed and connected to the grid with studding the side effects. Means that this integration affects the efficiency of the network and its continued service to the consumer, in addition to their impact in many respects related to power quality such as voltage profile, power factor and power loss based on standards. The Object of this study is to investigate the effect of connecting the up mentioned PV plants on the Tubas medium voltage networks as a case study and propose mitigation of these impact. A modelling of the case study was conducted using ETAP (Electrical Transient Analyzer Power) software where various solar PV penetration levels are added to the model and the power flow results are presented, which is the most comprehensive software used to design the integrated electrical systems. After propose the solution the first one add tap changer transformer and the second one add new feeder. The study results show that the voltage at the inter-connection point is enhanced through adding a tab changer transformer and the proposed new inter-connection point at a bus with suitable location. As a result of the simulation with adding Tap changer, it was found that the voltage fluctuation dropped to (3%) and the power losses to (14%). After adding the new feeder the voltage fluctuation reached up to (0.5%) and the losses to (5%). The results obtained were analyzed and presented in the study.

تقييم تأثير اتصال الأنظمة الكهروضوئية مع الشبكة على شبكة توزيع طوباس

زيادة استهلاك الطاقة الكهربائية والحاجة الفورية للكهرباء في فلسطين ، تقودنا إلى التفكير في تعزيز وتطوير نظام الطاقة الكهربائية. يعد استخدام أنظمة الطاقة المتجددة ، وخاصة الطاقة الشمسية ، أحد الطرق لإنتاج نظام طاقة كهربائية مستدامة وصديق للبيئة في فلسطين حيث تتمتع فلسطين بإمكانيات كبيرة من الإشعاع الشمسي. هناك ثلاثة محطات كهروضوئية تم تركيبها في ثلاثة مواقع مختلفة في شبكة طوباس ذات الجهد المتوسط وهي محطة مسلماني ومحطتان تشيكيتان ، 3 ميجاوات و 470 كيلوواط على التوالي،و يمكن أن يصل إجمالي انتاج الطاقة من أنظمة PV إلى 16٪ من الحمل الكلي. بنيت محطات الطاقة هذه دون دراسة الشبكة. يعني أن هذا التكامل يؤثر على كفاءة شبكة طوباس وخدمتها المستمرة للمستهلك في كثير من النواحي المتعلقة بجودة الطاقة مثل الجهد ومعامل تحسين القدرة و الطاقة الضائعة بناءً على معايير مختلفة. الهدف من هذه الدراسة هو دراسة تأثير توصيل المحطات الكهروضوئية المذكورة أعلاه على شبكات طوباس متوسطة الجهد كدراسة حالة. تم إجراء دراسة نموذجية لدراسة الحالة باستخدام برنامج ETAP حيث تمت إضافة مستويات اختراق الطاقة الشمسية الكهروضوئية إلى النموذج مع عرض نتائج تدفق الطاقة، وهو برنامج مناسب للغاية لتحليل تدفق الطاقة . تظهر نتائج الدراسة أن الجهد الكهربائي عند نقطة التوصيل الرئيسية قد تم تعزيزها من خلال إضافة محول تنظيم الجهد ونقطة ربط اضافية جديدة مقترحة في الموقع المناسب. بعد إضافة محول تنظيم الجهد وجد أن هذا يقلل من تذبذب التيار الكهربائي إلى (3٪) وفقدان الطاقة إلى (14٪). بعد إضافة وحدة التغذية الجديدة ، يصل تقلب الجهد (0.5٪) والخسائر إلى (5٪). تم تحليل النتائج وتقديمها في الدراسة.

DECLARATION

I declare that the Master Thesis entitled" **Assessment the Influence of Grid Connected Photovoltaic System on Distribution Network in Tubas**" is my own original work, and herby certify that unless stated, all work contained within this thesis is my own independent research and has not been submitted for the award of any other degree at any institution, except where due acknowledgement is made in the text.

Student Name: Yehya Nadi Hassouneh

Signature: Date:

STATEMENT OF PERMISSION TO USE

In presenting this thesis in partial fulfillment of the requirements for the joint Master's degree in Renewable Energy & Sustainability at Palestine Polytechnic University and Al-Quds University, I agree that the library shall make it available to borrowers under rules of the library.

Brief quotations from this thesis are allowable without special permission, provided that accurate acknowledgement of the source is made.

Permission for extensive quotation from, reproduction, or publication of this thesis may be granted by my main supervisor, or in his absence, by the Dean of Graduate Studies and Scientific Research when, in the opinion of either, the proposed use of the material is for scholarly purposes.

Any coping or use of the material in this thesis for financial gain shall not be allowed without my written permission.

Student Name: **Yehya Nadi Hassouneh**

Signature: Date:

DEDICATION

This thesis is dedicated to:

The sake of Allah, my Creator and my Master,

My great teacher and messenger, Mohammed (May Allah bless

and grant him), who taught us the purpose of life,

My homeland Palestine, the warmest womb;

The great martyrs and prisoners, the symbol of sacrifice;

The Polytechnic University, my second magnificent home;

My great parents, who never stop giving of themselves in countless ways,

My dearest wife, who leads me through the valley of darkness with light of hope and support,

My beloved brothers and sisters; particularly my dearest brother, Imad, who stands by me when things look bleak,

My beloved kids: Nadi, and Eleen , whom I can't force myself to stop loving. To all my family, the symbol of love and giving,

My supervisor Prof . Abdel-Karim Daud

My friends who encourage and support me (Haitham ALqadi)

All the people in my life who touch my heart,

I dedicate this research.

ACKNOWLEDGEMENT

I would like to express my gratitude for everyone who helps me during this master thesis, starting with endless thanks for my supervisor Prof. Abdel-Karim Daud who didn't keep any effort in encouraging me to do a great job, providing me with valuable information and advice to be better each time. Thanks for the continuous support and kind communication which great effect regarding to feel interesting about what I am working on. Thanks are extended to the program coordinator Prof. Sameer Khader for his efforts towards the success of the program, many thanks for Eng Haitham AlQadi, whose helped me with them useful notes, which support my work. Also my thanks are extended to all instructors and engineers who helped me during the first stages of my master thesis.

I would like to thank JAMILA Project-544339-TEMPUS-1-2013-1-IT-TEMPUS-JPCR funded by the European Union which was administrated by Sapienza University of Rome and partner Universities for their support in launching this program, provided infrastructure and opportunities for scientific visits.

Finally, my ultimate thanks go to the great edifice of science (Palestine Polytechnic University).

TABLE OF CONTENT

LIST OF FIGURES

LIST OF TABLES

LIST OF ABBREVIATIONS

AC	Alternative Current
DC	Direct Current
DG	Distributed Generation
ECP	Electrical Connection Point
ECP	Energy Connection Point
ETAP	Electrical Transient Analysis Program
IEC	Israel Electrical Company
IEEE	Institute Electrical and Electronics Engineer
IEEE-SA	The Institute of Electrical and Electronics Engineers Standards Association
KWh	Kilo Watt Hour
LTC	Load Tap Changer
MPPT	Maximum Power Point
MV	Medium Voltage
PCC	Point of Common Coupling
PF	Power Factor
PSH	Peak Sun Hour
PV	Photovoltaic
PV-syst	Software PV-syst
SLD	Single Line Diagram
SPV	Solar Photovoltaic
TEDCO	Tubas Electrical Distribution Company
THD	Total Harmonic Distortion

LIST OF SYMBOLS

ΔP_i	The Difference Active Power
ΔQ_i	The Difference Reactive Power
B_{Voc}	Open Circuit Temperature Coefficient
B_{ik}	Imaginary Part of the Element in the YBUS
G_{ik}	Real Part of The Element in the YBUS
$\lvert V \rvert$	Voltage Magnitude
$\Delta\theta$	Phase Shrinking Angle
I	Output Current
I_{mp}	Current at Maximum Power Point
Io	Saturation Current of the Diode
I_{SC}	Short Circuit Current
I_{sh}	Short Circuit Temperature Coefficient
J	Jacobian Matrix
k	Boltzmann Constant
Mvar	Mega Volt Amper (Reactive Power)
N	Number of Buses
n	Curve Fitting Constant
PD	Real Power
Pi	Net Power at Bus
p_{mp}	Power at Maximum Point
pu	Per Unit
q	Electron
QD	Reactive Power
R	Number of Generator

Tr	Absolute Temperature
Vg	Gap Voltage
V_{mp}	Voltage at Maximum Power Point
Vo	Voltage on the Shunt Resistance
V_{OC}	Open Circuit Voltage
V_{sc}	Voltage Source Converter
X/R	Ratio of a Transformer is Simply the Imaginary of its Impedance
YBUS	Bus Admittance Matrix
Z%	Percentage of Rated Voltage Applied to the Transformer

1

Chapter 1: Introduction

1.1 Overview

1.2 Objectives

1.3 Motivations

1.4 Problem Formulation

1.5 Methodology

1.1 Overview

The increasing of pollution caused by fuel combustion has become a serious concern for the ecosystem. The world is turning to use the renewable energy, which is considered sustainable and environmentally friendly especially in generating electricity, while traditional methods of power generation have become less used. Now the world depending has become on solar, wind and other environmentally friendly sources, which represent distribution generator (DG). One of the most widespread sources in the world, especially in Palestine, is solar energy. However, it causes problems in distribution networks. In this thesis, we are going to explain how these problems affect the grid by focusing on a case study selected.

1.2 Objectives

1- Power flow analysis.
2- Study the voltage fluctuation.
3- Power factor effect.
4- Power losses analysis.
5- PV plant analysis.
6- Power consumption of case study network.
7- Analysis of the Tubas medium voltage network through the ETAP software and by using real data.
8- Study the best way to increase the reliability of the network.

1.3 Motivations

One of the advantages of the spreading of the PV and its connection with the grid is that it reduces the dependence on the conventional energy source which causes many environmental problems. The PV generation is increasingly widespread in the distribution network but quality problems have been detected that may affect the operation of the network, which is a very big challenge [1].

1.4 Problem Formulation

Distribution generation (DG) resources, when implemented in a large scale without any specialized controls, are found to impact the integrity, reliability, security and the stability of the power grid. Electrical distribution systems are undergoing continuous changes with respect to increase penetration of renewable energy sources. The integration of source such as solar PV poses various challenges in the system [2,3]. Some major challenges are voltage unbalance [2], Voltage rise [4], Reverse power flow [5], Power factor and Harmonics.

1.5 Methodology

1- Select the case study and collecting the data of the PV and load.
2- Creating the single line diagram for 33 kV network.
3- Simulation of the PV stations (plants) on the PV-syst software.
4- Building and analyzing the network by ETAP software.
5- Power flow analysis.
6- Getting the suitable and required information and statistics from the ETAP Program reports.
7- Feasible scenarios for developing and improving the network.

1.6 Thesis Structure

This research is divided into five chapters. The previous studies that deals with the impact of Grid connected photovoltaic system in the medium voltage network and make modeling for all component of the network are given in chapter 2. A case study of Tubas electrical network with PV integration and the network modelling are given in Chapter 3. Chapter 4 includes Simulations: Results and Discussions using ETAP software. In Chapter 5, will proposed a method to enhance the performance of Tubas network based on the simulation and includes the conclusions and future work for this study.

2

Chapter 2: Impact of Grid Connected Photovoltaic System on the Medium Voltage Network

2.1 Introduction

In the past decade, traditional and unsustainable sources of energy pose a major threat to ecosystem. The world now devotes all its resources to find solutions to this problem and to increase reliance on renewable and clean energy. Photovoltaic (PV) technology is one of these solutions. A photovoltaic (PV) system comprises a semiconductor panel converting sunlight into direct current electricity and an inverter converting direct current to alternative current used in the grid [6].

Since Palestine is occupied and all the possibilities controlled by the occupation, and the increase in the demand for electricity is very large and there is some shortages in peak load hours, so the demand for installation of solar systems and the reliance on the deployment of PV systems has been increasing significantly due to supportive policies in Palestine, the PV deployment in which the systems are installed geographically near consumers scattered throughout the grid. Renewable energy resources when implemented in large scale without any specialized controls is found to impact the integrity reliability security and stability of the power grid.

The problem, nonetheless, cannot be solved easily as a new problem arises from the variable and intermittent nature of solar power. Even if we assume the most optimistic situation in which the weather and the panels always have an uninterrupted view of the sun, the power generated from the PV power system changes drastically throughout a day. When the sunlight is shading by clouds or from surroundings, the power from the PV system can be dropped sharply. Unlike mechanical based electricity generation, PV generation has no inertia that smooths the power output. As a result, any PV generation, including the distributed one, provides more volatile power than the current load from consumers and power from generators. If there is a high level of distributed PV generation in the grid, the characteristic of the net load will be significantly distorted from the normal load. Then the grid operator may not be able to balance with the current set of supply infrastructures. The current level of PV generation is not yet sufficient to cause a problem to grid operators. With the high rate of the increasing distributed PV deployment, it is a must that understand the limits of PV generation.

The commonly used PV model for each individual PV system consist of multiple steps including finding solar irradiance in the sky, projecting solar irradiance to the panel, determining DC power output from the panel, and converting the power output compatible to the grid [7].

The impact of PV integration can be listed as follows voltage variations and unbalance, current and voltage harmonics, grid islanding protection, and other power quality issues, the PV integration lead to some of the PV integration effects can be listed as follows, flicker and stress on distribution transformer [8,9].

The power flow study also known as load-flow study is an important tool involving numerical analysis applied to a power system. Unlike traditional circuit analysis, a power flow study usually uses simplified notation such as a single line diagram and per-unit system, and focuses on various forms of AC power (i.e. reactive, real, and apparent) rather than voltage and current. It analyzes the power systems in normal steady-state operation.

In this chapter a model of an existing electrical network taking care of all the parameters required for the simulation and analysis. With the help of Tubas Grid, the Tubas 33KV network in modeled using electrical transient analysis power ETAP software. Load flow study is carried out using Newton Raphson method (NRM) and voltage profile of buses are analyzed.

2.2 PV System as Distribution Generators

Distributed generation refers to a variety of technologies that generate electricity at or near where it will be used, such as solar panels and combined heat and power. Distributed generation may serve a single structure, such as a home or business, or it may be part of a micro-grid (a smaller grid that is also tied into the larger electricity delivery system), such as at a major industrial facility, or a large college campus. When connected to the electric utility's medium voltage distribution lines, distributed generation can submit clean energy and also reliable power to additional customers and reduce electricity losses along transmission lines. However there are many common distributed generation systems all over the world, which generate electricity from conventional or renewable sources such as:

- Solar photovoltaic systems.
- Wind turbines.
- Natural-gas-fired fuel cells.
- Combined heat and power systems.
- Hydropower.
- Biomass combustion.

- Municipal solid waste incineration.

Distributed generation can benefit the environment if its use reduces the amount of electricity that must be generated at centralized power plants, which result in reducing the environmental impacts of centralized generation. By using local energy sources, distributed generation reduces or eliminates the “line loss” that happens during transmission and distribution in the electricity delivery system [6].

According that in this thesis will focus on the three PV systems we will be dealing with as DG in Tubas, whereas will make modeling and analysis for power flow to study the effect of PV-grid connected.

2.3 Impact of DG on Distribution Networks

The effect of the DG still had not significant impact if the rate of DG is low [5] , but on the large scale and the amount of DG increase the effect of the grid problems such as harmonics, voltage fluctuation and frequency. These units could lead to some technical challenges. To mitigate some of these problems the solution are mentioned in [10].

- Power control parameters (power factor, fluctuation in power produced etc.)
- DG units not complying with utility protection rules.
- Islanding operation.

2.3.1 Voltage Fluctuation and Voltage Regulation Problem

High penetrations of PV can impact network voltage in a number of ways. Voltage rise and voltage variations caused by fluctuations in solar PV generation are two of the most prominent and potentially problematic impacts of high penetrations of PV. These effects are particularly pronounced when large amounts of solar PV are installed near the less loaded feeders [11].

Voltage quality can be affected by the intermittency of PV power output in distribution system [12]. Generally, for PV generation type, climate changes can create irradiance fluctuations either for a short or long period of time. Therefore, this can affect the voltage output of PV in Point of Common Coupling (PCC). The voltage problem of distribution system that has been connected with PV can be characterized as voltage rise, voltage unbalance and flickers in the network.

Fig.2.1 shows the voltage profile on the medium voltage (MV) feeder during light load and the maximum nominal load conditions with and without PV introduced power environment. As the off-load tap is already synchronized with approximating drop in voltage at maximum nominal load, hence voltage rise needs to examined only under light loads [13].

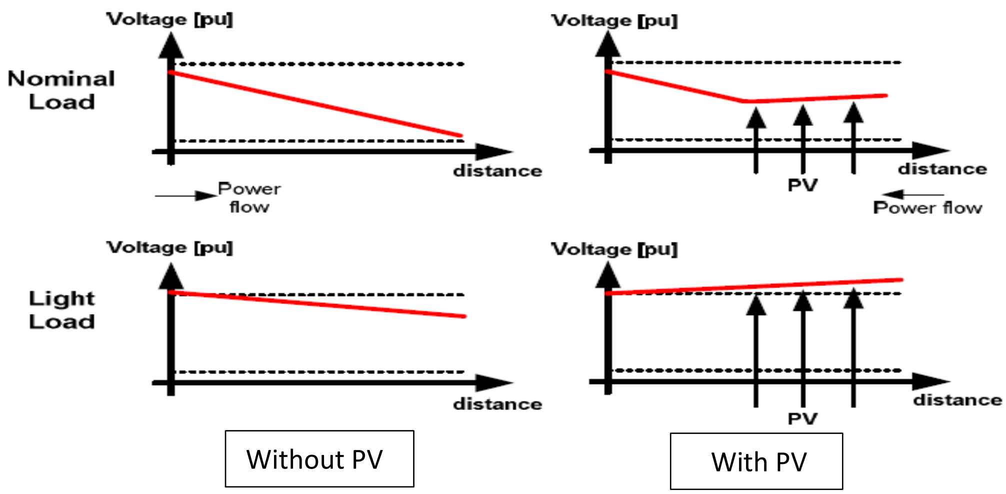

Fig.2.1 Typical voltage profile in a MV feeder with and without PV inverter [13]

2.3.2 Active and Reactive Power

The existing standards for PV-inverter interconnection mandates all inverters in grid-interface mode to function at unity power factor i.e. the inverter is not allowed to regulate voltage by consuming or generating reactive power. Numerous researchers have suggested that, these standards will not be practical for allowing high PV penetration levels on distribution network as the current regulation equipment is insufficient to control two-way power flows and very slow to match the rapidly moving cloud transients.

Normally, the real power loss reduction draws more attention for the utilities, as it reduces the efficiency of transmitting energy to customers. Nevertheless, reactive power loss is obviously not less important. This is due to the fact that reactive power flow in the system needs to be maintained at a certain amount for sufficient voltage level. Consequently, reactive power makes it possible to transfer real power through transmission and distribution lines to customers [14]. Can be reduce by strategically placed DG along the network feeder can be very useful if the decision maker is committed to reduce losses and to improve network performance by maintaining investments to a reasonable low level [15].

2.3.3 Power Losses

The main purpose of installing DG on a distribution system is to reduce power losses on the power system. One of the problems in power systems that can be solved by the installation of DG, will be explored in the use of DG in this study is to reduce the power loss in the transmission line. The simulation results from specific case studies on the IEEE 30 bus standard system shows that the power system loss was decreased from 5.7781 MW to 1,5757 MW or just 27,27% [16]. The methodology of less reduction increase is using DG by strategic location and capacity.

2.3.4 Power Factor

The power factor values are always above 0.85 and only fall below this number at high level of load, power factor decreases to unacceptable levels during PV system operation. When PV system works with high power values close to the rated, most active power demanded by the customers is supplied by the PV plant. Reducing the demand of active power from the grid, while reactive power demand is the same, result in low power factor measured at the substation [1].

2.4 IEEE Standard for PV-Grid Integration

The institute of electrical and electronics engineers standards association (IEEE-SA) is an organization within IEEE that develops global standards in a broad range of industries, including: power and energy, biomedical and health care, information and robotics, telecommunication and home automation transportation and many more.

In this section the standard power flow should be within the voltage, frequency, active and reactive power and power factor.

2.4.1 Voltage

With an increasing penetration of distributed generation (DG) deviations in the distribution network voltage may occur as a consequence of changes, and even reversal, of the power flow in the feeders. In high voltage networks the voltage is normally controlled through reactive power that causes an in-phase voltage component across the reactance of the line. In distribution networks the feasibility of voltage control with reactive power is limited due to the low X/R ratio. A solution is proposed, which is based on the insertion of a controllable inductance in the feeder. In combination with reactive power support of the DG units the voltage can be controlled [17]. DVAR can be utilized and the table below2.1 explain issue.

Table 2.1 Voltage range

Supply Voltage Variation		
VDE-AR-N 4015 Germany[18]	RD 661/2007 Spain[19]	Arrete 2011 France [20]
0.8 Un <1.1Un	0.85Un<U<1.1Un	0.9Un<U<1.1Un

The standards for voltage fluctuations at the point of connection of the PV plant facility to the power system should, for example, follow the requirement outlined in table 2.2.

Table 2.2 Voltage fluctuation limit

Voltage change	**Maximum rate of occurrence**
+/-3% normal level	Once per hour
+5/-6% of normal level	Once per 8-hour
Exceeding +5/-6%	As agreed by utility

2.4.2 Frequency

The PV plant control of the frequency, shouldn’t actively participate in primary frequency control during under-frequency. Having a “regulator like” control for a PV plant control scheme is a technical possibility and even desirable.

Table 2.3 Frequency range versus time

Frequency range (Hz)	**Time (second)**
>51.7	0
51.6 to 51.7	30
50.6 to 51.6	180
>49.4 to 50.6	Continuous operation
>48.4 to 49.4	180
>47.8 to 48.4	30

2.4.3 Power Factor

A PV plant at its full load, should be capable of 0.90 PF lagging and 0.95 PF leading. Automatic voltage regulation that is able to regulate the voltage at this point to a “desired” set-point should be within +/-0.5 %.

2.5 Modeling

This section will explain the power system modeling for Tubas network by using real information. For this purpose, Tubas power system (TEDCO) has been represented and a single line diagram is modeled using Electrical Transient Analyzer Programmed (ETAP) software. Load flow study is carried out in ETAP using Newton Raphson method and voltage profile of buses are analyzed. All of the physical and electrical parameters of the power system including height of towers, spacing between transmission lines, resistance and reactance values of transmission lines, transformer and power grid rating etc. A collected and applied to obtain the exact grid model of the power system. Then load flow study is conducted using ETAP and simulation results are studied. From the results of simulation, the buses with low voltage profiles are identified and possible solutions for improving the voltages are studied and their effectiveness is checked using this software [21].

Newton-Raphson Solution Method

There are several different methods of solving the resulting nonlinear system of equations. The most popular is known as the Newton-Raphson Method. This method begins with initial guesses of all unknown variables (voltage magnitude and angles at Load Buses and voltage angles at Generator Buses). Next, a Taylor Series is written, with the higher order terms ignored, for each of the power balance equations included in the system of equations. The result is a linear system of equations that can be expressed as:

$$\begin{bmatrix} \Delta\theta \\ \Delta|V| \end{bmatrix} = -J^{-1} \begin{bmatrix} \Delta P \\ \Delta Q \end{bmatrix} \tag{2.1}$$

$$\Delta P_i = -P_i + \sum_{k=1}^{N} |V|_i |V|_k (G_{ik} \cos\theta_{ik} + B_{ik} \sin\theta_{ik}) \tag{2.2}$$

$$\Delta Q_i = -Q_i + \sum_{k=1}^{N} |V|_i |V|_k (G_{ik} \cos\theta_{ik} - B_{ik} \sin\theta_{ik}) \tag{2.3}$$

$$J = \begin{bmatrix} \frac{\partial \Delta P}{\partial \theta} & \frac{\partial \Delta P}{\partial |V|} \\ \frac{\partial \Delta Q}{\partial \theta} & \frac{\partial \Delta Q}{\partial |V|} \end{bmatrix} \tag{2.4}$$

Where ΔP and ΔQ are called the mismatch equations and J is a matrix of partial derivatives known as a Jacobian.

The linearized system of equations is solved to determine the next guess (m + 1) of voltage magnitude and angles based on,

$$\theta^{m+1} = \theta^{m} + \Delta\theta \tag{2.5}$$

$$|\mathrm{V}|^{m+1} = |\mathrm{V}|^{m} + \Delta|\mathrm{V}| \tag{2.6}$$

The process continues until a stopping condition is met. A common stopping condition is to terminate if the norm of the mismatch equations are below a specified tolerance. Outline of solution of the power flow problem is:

1. Make an initial guess of all unknown voltage magnitudes and angles. It is common to use a "flat start" in which all voltage angles are set to zero and all voltage magnitudes are set to 1.0 p.u.
2. Solve the power balance equations using the most recent voltage angle and magnitude values.
3. Linearize the system around the most recent voltage angle and magnitude values.
4. Solve for the change in voltage angle and magnitude.
5. Update the voltage magnitude and angles.

Check the stopping conditions, if met then terminate, else go to step 2.

2.5.1 Modeling of Network

In the power flow problem, it is assumed that the real power PD and reactive power QD at each Load Bus are known. For this reason, Load Buses are also known as PQ Buses. For power grid buses, it is assumed that the real power generated PG and the voltage magnitude |V| is known. In electrical power systems a slack bus (or swing bus), defined as a V θ bus, is used to balance the active power |P| and reactive power |Q| in a system while performing load flow studies. The slack bus is used to provide for system losses by emitting or absorbing active and/or reactive power to and from the system. For the Slack bus, it is assumed that the voltage magnitude |V| and voltage phase θ are known. Therefore, for each Load Bus, the voltage magnitude and angle are unknown and should be solved; for each Generator Bus, the voltage angle must be solved for; there are no variables that must be solved for the Slack Bus. In a system with N buses and R generator or power grid, there are then 2 (N − 1) − (R − 1) unknowns.

In order to solve for the 2(N − 1) − (R − 1) unknowns, there must be 2(N − 1) − (R − 1) equations that do not introduce any new unknown variables. The possible equations to use are power balance equations, which can be written for real and reactive power for each bus. The real power balance equation is:

$$0 = -P_i + \sum_{k=1}^{N} |V|_i |V|_k (G_{ik} \cos\theta_{ik} + B_{ik} \sin\theta_{ik}) \tag{2.7}$$

where P_i is the net power injected at bus i, G_{ik} is the real part of the element in the bus admittance matrix YBUS corresponding to the i_{th} row and kth column, B_{ik} is the imaginary part of the element in the YBUS corresponding to the i_{th} row and kth column and θ_{ik} is the difference in voltage angle between the ith and kth buses. The reactive power balance equation is:

$$0 = -Q_i + \sum_{k=1}^{N} |V|_i |V|_k (G_{ik} \cos\theta_{ik} - B_{ik} \sin\theta_{ik}) \tag{2.8}$$

Equations included are the real and reactive power balance equations for each Load Bus and the real power balance equation for each Generator Bus. Only the real power balance equation is written for a Generator Bus because the net reactive power injected is not assumed to be known and therefore including the reactive power balance equation would result in an additional unknown variable. For similar reasons, there are no equations written for the Slack Bus.

Fig.2.2 show the three phase line section between bus *x* and *y*. The line parameters are obtained by the technique developed by Carson and Lewis, considering the effects of self and mutual couplings of the unbalanced three phase line section, A 4 x 4 matrix can be expressed as (2.9). By the application of Kron's reduction technique, the resultant matrix is reduced to (2.10) [21].

$$[Z_{xy}^{abcn}] = \begin{bmatrix} Z_{xy}^{aa} & Z_{xy}^{ab} & Z_{xy}^{ac} & Z_{xy}^{an} \\ Z_{xy}^{ba} & Z_{xy}^{bb} & Z_{xy}^{bc} & Z_{xy}^{bn} \\ Z_{xy}^{ca} & Z_{xy}^{cb} & Z_{xy}^{cc} & Z_{xy}^{cn} \\ Z_{xy}^{na} & Z_{xy}^{nb} & Z_{xy}^{nc} & Z_{xy}^{nn} \end{bmatrix} \tag{2.9}$$

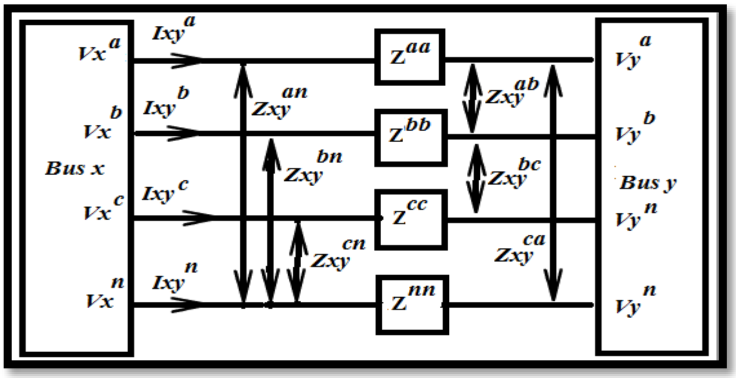

Fig 2.2: Representation of a 3-phase, 4-wire line section

$$[Z_{xy}^{abc}] = \begin{bmatrix} Z_{xy}^{aa-n} & Z_{xy}^{ab-n} & Z_{xy}^{ac-n} \\ Z_{xy}^{ba-n} & Z_{xy}^{bb-n} & Z_{xy}^{bc-n} \\ Z_{xy}^{ca-n} & Z_{xy}^{cb-n} & Z_{xy}^{cc-n} \end{bmatrix} \tag{2.10}$$

The relationships between bus voltages and branch currents for Fig.2.2can be given as (2.11), (2.12).

$$\begin{bmatrix} V_y^a \\ V_y^b \\ V_y^c \end{bmatrix} = \begin{bmatrix} V_x^a \\ V_x^b \\ V_x^c \end{bmatrix} - [Z_{xy}^{abc}] \begin{bmatrix} I_{xy}^a \\ I_{xy}^b \\ I_{xy}^c \end{bmatrix} \tag{2.11}$$

Above equation (2.11) can be written as

$$[V_{xy}^{abc}]=[Z_{xy}^{abc}][I_{xy}^{abc}] \tag{2.12}$$

Load Flow Data Requirement

1- Bus Data

Required data for load flow calculations for buses includes:

- Nominal kV
- %V and Angle (when Initial Condition is set to use Bus Voltages)
- Load Diversity Factor (when the Loading option is set to use Diversity Factor)

2- Branch Data

Branch data is entered into the Branch Editors, i.e., Transformer, Transmission Line, Cable, Reactor, and Impedance editors. Required data for load flow calculations for branches includes:

- Branch Z, R, X, or X/R values and units, tolerance, and temperature, if applicable
- Cable and transmission line, length, and unit
- Transformer rated kV and kVA/MVA, tap, and LTC settings
- Impedance base kV and base kVA/MVA

3- Power Grid Data

Required data for load flow calculations for power grids includes:

- Operating mode (Swing, Voltage Control, Mvar Control, or PF Control)
- Nominal kV
- %V and Angle for swing mode
- %V, MW loading, and Mvar limits (Q_{max} & Q_{min}) for Voltage Control mode
- MW and Mvar loading, and Mvar limits Mvar Control mode
- MW loading and PF, and Mvar limits for PF Control mode

4- Synchronous Generator Data

Required data for load flow calculations for synchronous generators includes:

- Operating mode (Swing, Voltage Control, or Mvar Control)
- Rated kV
- %V and Angle for swing mode of operation
- %V, MW loading, and Mvar limits (Q_{max} and Q_{min}) for Voltage Control mode
- MW and Mvar loading, and Mvar limits Mvar Control mode

2.5.2 Modeling of Load

A distribution system has a variety of 1-phase and 3- phase loads connected at the branches and laterals. These loads can be modeled as constant power (PQ), constant impedance, constant current and any combination of the above. Table 2.4 summarizes the model equations of the various loads[16].

Modeling load is a necessary task for energy scheduling and grid operation. At the level of substation and beyond, modeling load is relatively simple. While load at the level of household is volatile, aggregation of loads at the level of substations and the grid is likely to be smooth and predictable. Despite significant differences from day to day, modeling load at substation is accurate provided contingencies do not arise. An overview of the load pattern at substation, the grid and the different types of forecast needed in general operation will be discussed in detail throughout the study.

Table 2.4 Model equations of the various types of loads.

	Constant power (PQ)	Constant Impedance	Constant current
Wye connected load	$\begin{bmatrix} I_{L,a} \\ I_{L,a} \\ I_{L,a} \end{bmatrix} = \begin{bmatrix} \frac{(S_a)}{V_{an}} \\ \frac{(S_b)}{V_{bn}} \\ \frac{(S_c)}{V_{ac}} \end{bmatrix}$	$\begin{bmatrix} Z_a \\ Z_b \\ Z_c \end{bmatrix} = \begin{bmatrix} \frac{V_{an}{}^2}{S_b} \\ \frac{V_{bn}{}^2}{S_b} \\ \frac{V_{cn}{}^2}{S_c} \end{bmatrix}$ The load currents as a function constant load impedances are given as $\begin{bmatrix} I_{L,a} \\ I_{L,a} \\ I_{L,a} \end{bmatrix} = \begin{bmatrix} \frac{(V_{an})}{Z_a} \\ \frac{(V_{bn})}{Z_b} \\ \frac{(V_{cn})}{Z_c} \end{bmatrix}$	$\begin{bmatrix} I_{L,a} \\ I_{L,a} \\ I_{L,a} \end{bmatrix} = \begin{bmatrix} I_{L,a} < \delta_a - \theta_a \\ I_{L,b} < \delta_b - \theta_b \\ I_{L,c} < \delta_c - \theta_c \end{bmatrix}$ Where δ_{abc} are line-to- neutral voltage angles θ_{abc}power factor angles
Delta connected load	$\begin{bmatrix} I_{L,ab} \\ I_{L,bc} \\ I_{L,ca} \end{bmatrix} = \begin{bmatrix} \frac{(S_{ab})}{V_{ab}} \\ \frac{(S_{bc})}{V_{bc}} \\ \frac{(S_{ca})}{V_{ca}} \end{bmatrix}$	$\begin{bmatrix} Z_{ab} \\ Z_{bc} \\ Z_{ca} \end{bmatrix} = \begin{bmatrix} \frac{V_{ab}{}^2}{S_{ab}} \\ \frac{V_{bc}{}^2}{S_{bc}} \\ \frac{V_{ca}{}^2}{S_{ca}} \end{bmatrix}$ The load currents as a function constant load impedances are given as $\begin{bmatrix} I_{L,ab} \\ I_{L,bc} \\ I_{L,ca} \end{bmatrix} = \begin{bmatrix} \frac{(V_{ab})}{Z_{ab}} \\ \frac{(V_{bc})}{Z_{bc}} \\ \frac{(V_{ca})}{Z_{c}a} \end{bmatrix}$	$\begin{bmatrix} I_{L,ab} \\ I_{L,bc} \\ I_{L,ca} \end{bmatrix} = \begin{bmatrix} I_{L,ab} < \delta_{ab} - \theta_{ab} \\ I_{L,bc} < \delta_{bc} - \theta_{bc} \\ I_{L,ca} < \delta_{ca} - \theta_{ca} \end{bmatrix}$ Where δ_{abc} are line-to- neutral voltage angles θ_{abc}power factor angles

Fig.2.3 Summaries the load flow approach using Newton Raphson method.

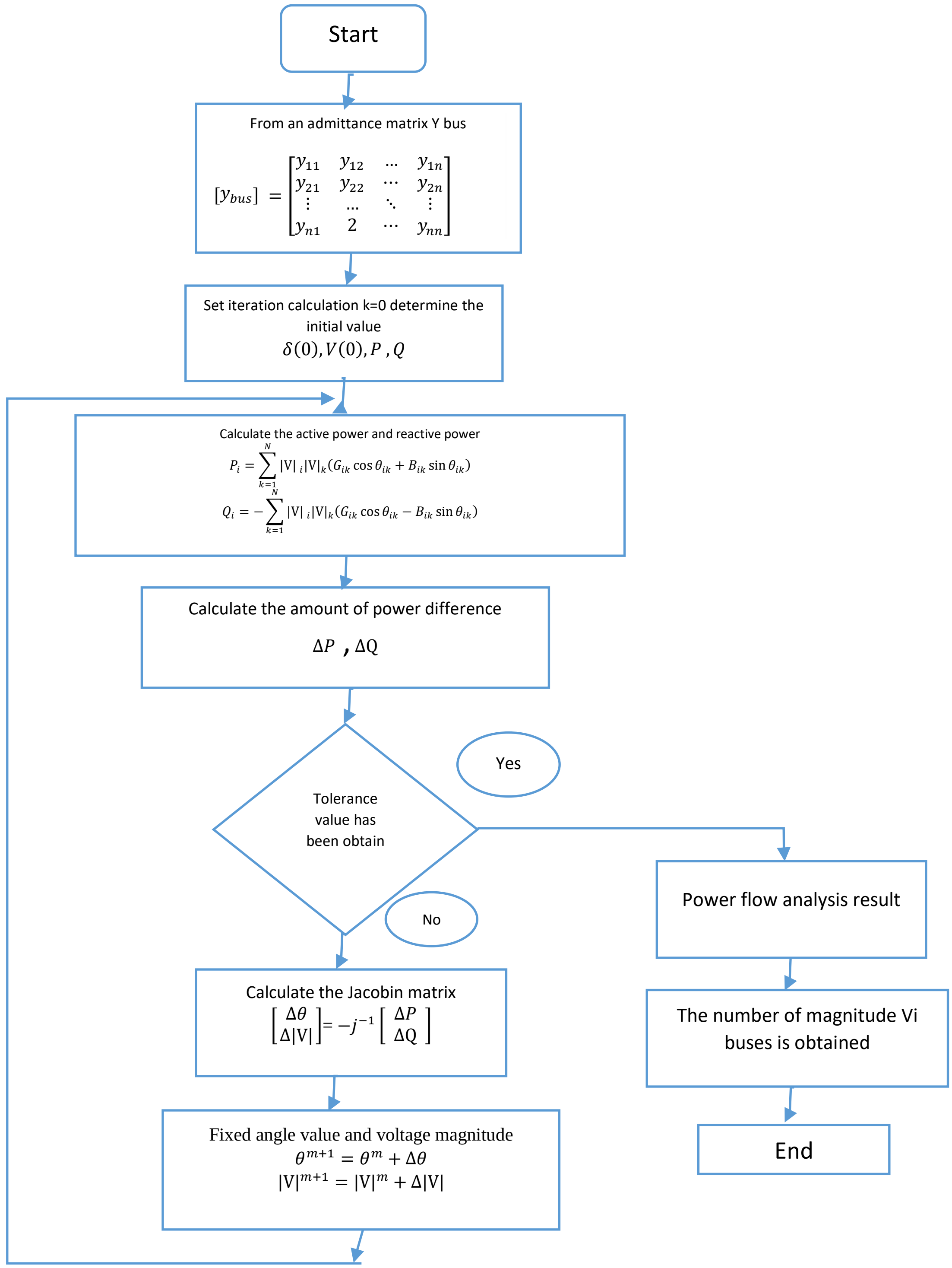

Fig.2.3 Flowchart calculation of power flow using Newton Raphson method

2.5.3 Modeling of PV

The fundamental components of a grid-connected PV systems consist of a series/parallel mixture of PV arrays to directly convert the sunlight to DC power, and a power-conditioning unit that converts the DC power to AC power, and also keeps the PVs operating at the most efficient point [22].

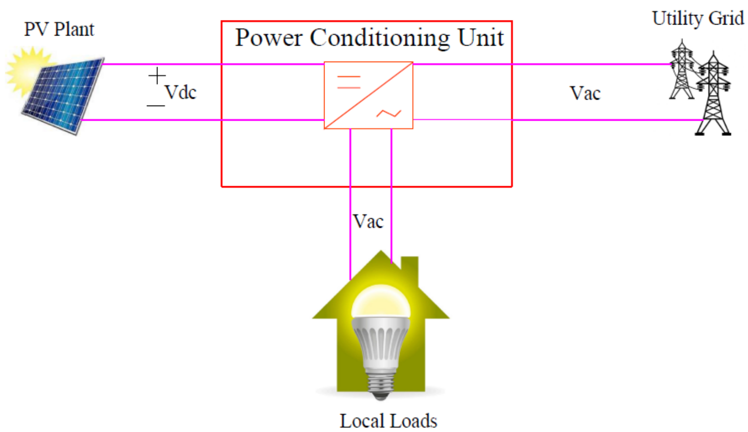

Fig.2.4 General diagram of the grid-connected PV systems.

Generally, the electric characteristics of a PV unit can be expressed in terms of the current-voltage, or the power-voltage relationships of the cell. The variations of these characteristics directly depend on the received solar irradiation and the cell temperature. Therefore, to analyze the dynamic performance of PV systems under different weather conditions, an accurate model is required to convert the effect of irradiance and temperature variations on the produced current and voltage of the PV arrays. Fig.2.5 shows the equivalent electrical circuit of a typical PV cell, where I is the output terminal current, I_L is the light-generated current, I_d is the diode current, I_{sh} is the shunt leakage current, R_s is the internal resistance, and R_{sh} is the shunt resistance.

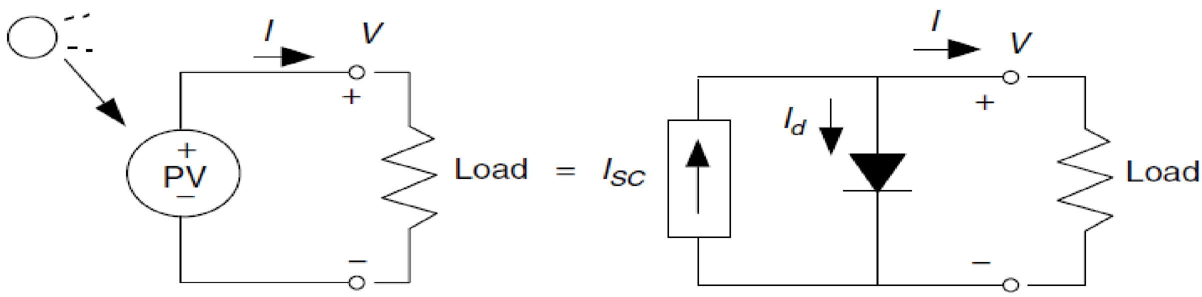

Fig.2.5 Equivalent electrical circuit of a typical PV cell

From Fig 2.5, the output current, *I* of the PV module can be express as,

$$\mathrm{I} = I_{sc} - I_d \quad (2.13)$$

Where *Vo* is the voltage on the shunt resistance. The diode current, I_d can be obtain using classical diode current expression as [23].

$$I_d = I_0\,[e^{\frac{qV_{oc}}{\mathrm{KT}}} - 1] \quad (2.14)$$

Where *Io* is the saturation current of the diode, q is electron, *K* is Boltzmann constant, T is temperature on absolute scale 25$^{\mathrm{O}}$C. By substituting (2.14) in (2.13) and ignoring the last term, the output current, *I* can be rewritten as,

$$\mathrm{I} = I_{sc} - I_0\,[e^{38.9V} - 1] \quad (2.15)$$

Where, the saturation current I_0 at different operating temperature can be calculated as [24] ,

$$V_{oc} = V_{oc} * (1 + \beta_{V_{oc}}[\mathrm{T} - 25]) \quad (2.16)$$

Where, $\beta_{V_{oc}}$is the open circuit temperature coefficient, Using the provided coefficient by manufacturers and the mathematical equations, any PV module can be modelled for dynamic analysis. The produced DC voltage of PV module can be raised to any desired level using a DC-DC boost converter and MPPT technique can be used in the boost converter to efficiently control the produced power of PV arrays. The produced DC power is then converted to AC power using a three-phase three-level Voltage Source Converter (V_{SC}) and injected to the system using a coupling transformer.

3

Chapter 3: Case study of Tubas Electrical Network with PV Integration

3.1 Introduction

3.2 Case Study Description

3.2.1 Tubas Substation

3.2.2 Distribution the PV Station in Palestine

3.2.3 Single Line Diagram of the Tubas

3.2.4 Case Study Specification

3.2.5 Load Demand Specification

3.4 Load Demand Specification

3.3 Description of PV Systems

3.3.1 Maslamani PV Plant

3.3.2 Czechia Plant (350 and 120) kW

3.1 Introduction

The main goal of an electric grid operation is to supply electric energy from generators to customers that satisfies the electrical demand, so it should be taken into consideration the maximum load and the all safety conditions .In a grid operation, an electric power produced by generators called a generated power or supply must be equal to an electric power required by consumers called a load or demand at all times. The grid operation is facing complicated conditions produced from a large number of non-linear constraints coming from operational limits in generators such as transmission networks, distribution networks, and customer units. The reliability of components in the grid also makes the grid operation complicated. Another source of complication is an uncertainty in loads. Once a high amount of distributed PV generation is added to the demand side as a negative load, the net load which is a summation of a regular load and a negative load become even more uncertain.

Studies and actual operating experience indicate that it is easier to integrate PV solar energy into a power system where other generators are available to provide balancing power, regulation and precise load-following capabilities. The higher the degree of distributed generation of solar farms operating in a given area, the less their aggregate production will be variable.

Integration of solar photovoltaic (PV) resources in high penetration level may introduce a multitude of adverse impacts on grid operation. Voltage rise, reverse power flow, voltage unbalance can be listed as some of the major impacts.

In this chapter, the distribution network of Tubas will be described in addition to all real parts and information of network parts. Moreover, an accurate study the influences of installed large grid-connected PV systems on the dynamic performance of distribution networks will be discussed too. To investigate the effects of different weather conditions on the produced power of the PV modules, required meteorological data related to tubas for one year are collected from the TEDCO.

3.2 Case Study Description

The purpose of this chapter is to study the full details of the Tubas network, where all data will be included to the simulation program.

3.2.1 Tubas Substation

The proposed power flow approach is a test done on a real distribution feeder in Tubas in north Palestine. Tubas Electricity Distribution Company (TEDCO) is one of the leading companies in the field of distribution generation especially solar systems. Since the beginning of 2013, the large number of applications submitted by the citizens of Tubas Electricity Company to install solar power generation units.

In recent years, large solar power plants had been installed in Tubas, without studying the effects on the electrical grid medium voltage (MV). Fig.3.1 represents the block diagram for grid-connected PV system.

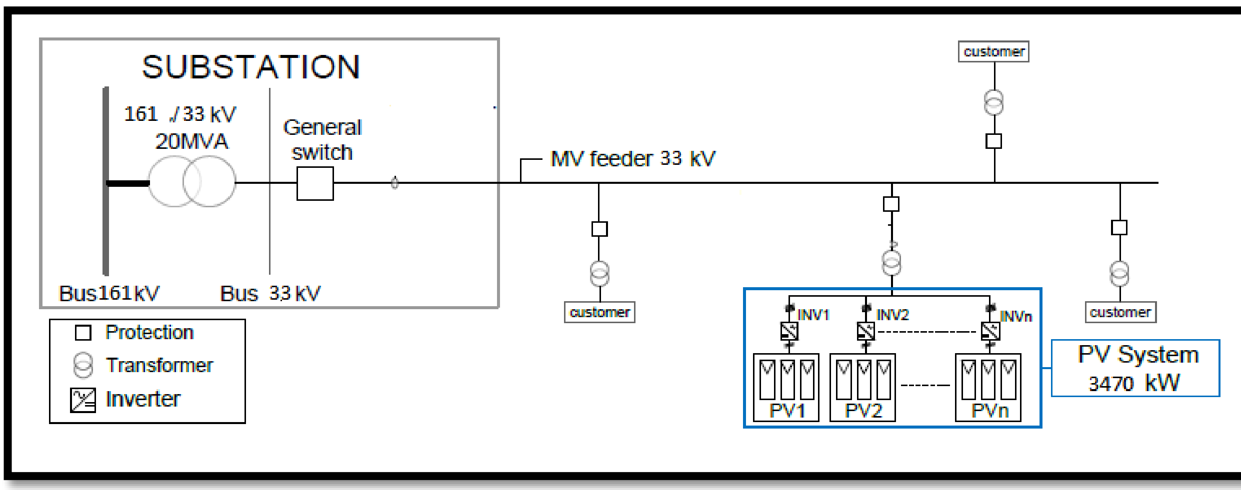

Fig.3.1 Schematic block circuit diagram of the PV-grid tie system.

3.2.2 Distribution the PV Station in Palestine

Palestine is situated between (29.15º – 33.15º) north latitude and (34.15º – 35.14º) longitude east which is an ideal location for solar energy utilization. Tubas is situated at 32.19º latitude and 35.29º longitude. The daily average solar radiation varies between (2.83 to 8.5) kWh per square meter/day. Maximum amount of radiation is available during the month of June -July and minimum on December-January.

Monthly global solar insolation and daily average bright sunshine hours in Tubas city are presented in the table 3.1. These values are a 22-year ago average solar insolation from the PV-syst software.

Table 3.1: Monthly global solar insolation at Tubas [28]

Month	**Solar insolation (kWh/m^2-day)**
January	2.69
February	3.2
March	4.95
April	6.2
May	7.27
June	8.2
July	7.8
August	7.7
September	6.27
October	4.35
November	3.5
December	2.75
Total PSH/year	64.88
Average insolation	**5.4**

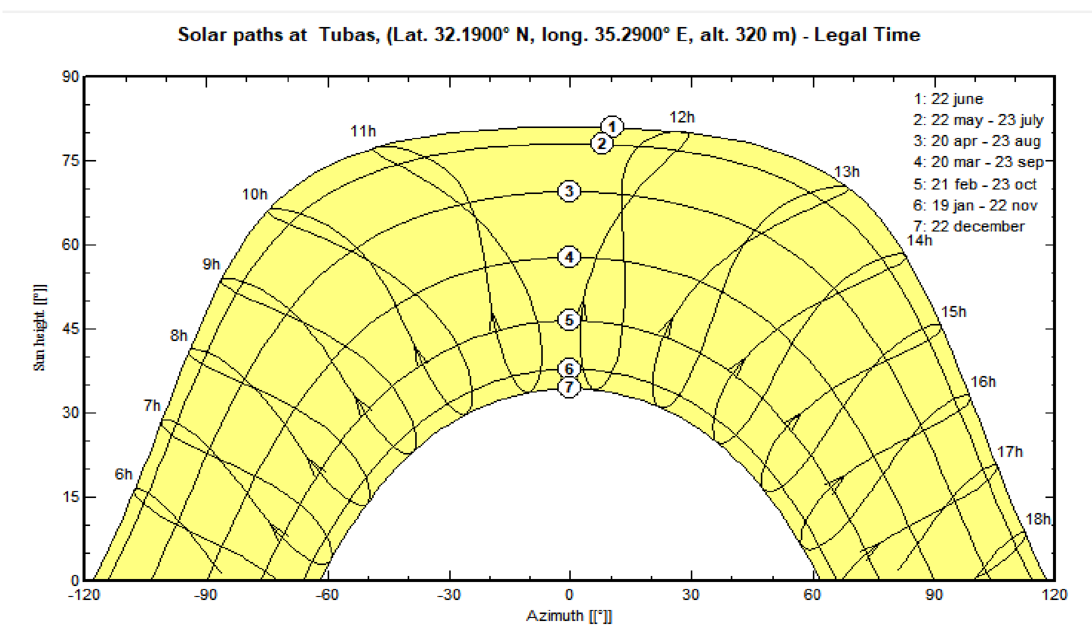

Fig.3.2 Solar path at Tubas, (Lat.32.19º N, Long. 35.29º, alt. 350 above sea level)

Measured data of both situations (with and without PV generation). The line studied is a rural distribution grid of 33 kV in the Tubas with an approximated installed power of 3.5 MW that supplies to 115 customers, including a small town and also many dispersed irrigated farms. The line is connected to a 20 MVA transformer in a substation with one level of voltages 33 kV.

3.2.3 Single Line Diagram of the Tubas

Fig.3.3 shows the single line diagram (SLD) for Tubas network. Bus 1 and 2 are considered as power grid bus, 3-55 is considered as load bus. SLD representative of the Tubas grid and how the different loads and PV plants are interconnected can be found below. The diagram also shows the protective equipment for the system, avital necessity in the power industry.

SLD contain a large number of the buses as shown in **appendix A**, therefore will be studied a bunch of buses around the solar plants down to the main station (Tyaseer interconnection point) as shown in Fig.3.3. The networks are simplified in another parts are assumed as a lump load.

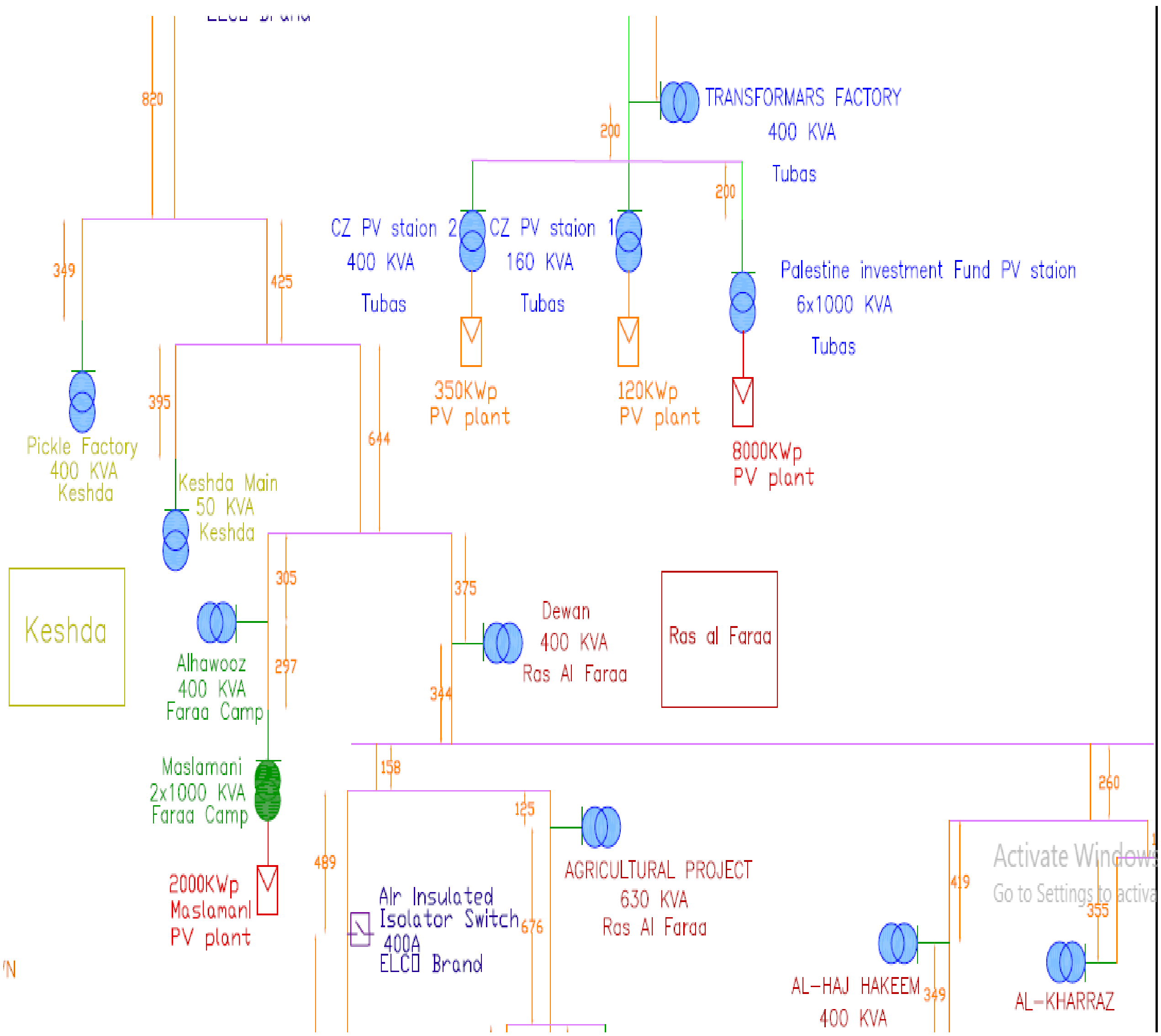

Fig.3.3 Practical distribution feeder single line diagram of the tubas

3.2.4 Case Study Specification

The 55-bus system is a standard distribution test feeder to verify power flow programs with different transformer connection. The unbalanced loading scenario with delta-wye step down transformer connection is used in this Distribution line. The 33 kV line segment is configured as 3-wire and the 0.4 kV segment is configures as 4-wire.

The test feeder is an 80 km 33 kV without any voltage regulators. The 0.4 kV LV feeders are connected at different buses along the MV feeders through 33/0.4 kV delta-wye transformers. Residential loads in the LV feeders are distributed in an unbalance pattern among the phases. The line is connected to a 20 MVA transformer in a substation with two levels of voltages 161 kV/33 kV.

3.2.5 Load Demand Specification

There are many parameter to evaluate the PV influence on the grid which are size and the peak power of the PV system, the rated power and the short circuit power of the grid. All of them are related to the PV power penetration level [10], in order to study of the effect of PV on grid, the worst case should be studied. In this example, the worst case is the month of July where the highest load with the PV production occurs.

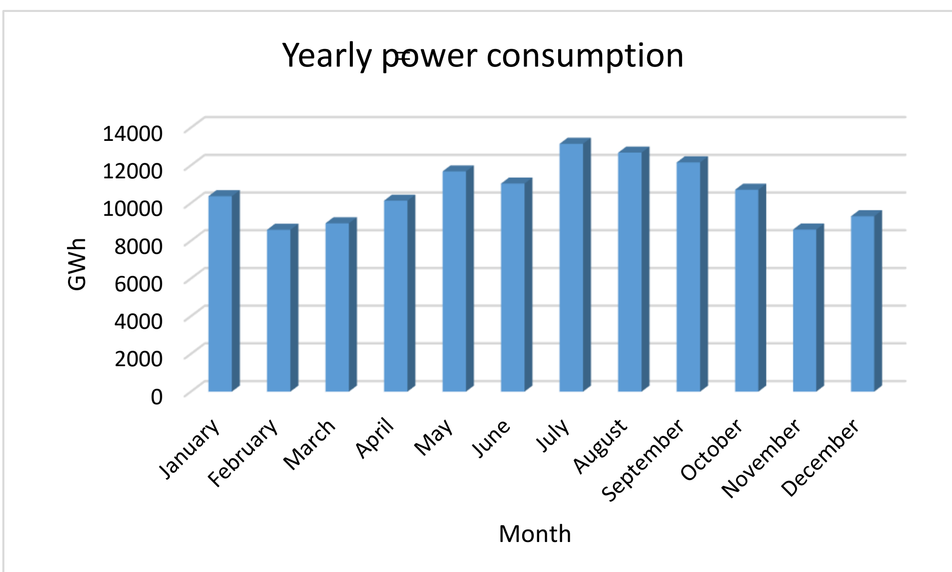

Fig.3.4 Monthly consumption of the Tubas station within 2017

It's worth mentioning that the capacity of Tubas station is 20 MVA. The data clearly shows that the demand for electricity is increasing significantly year after year as shown in Fig.3.5.

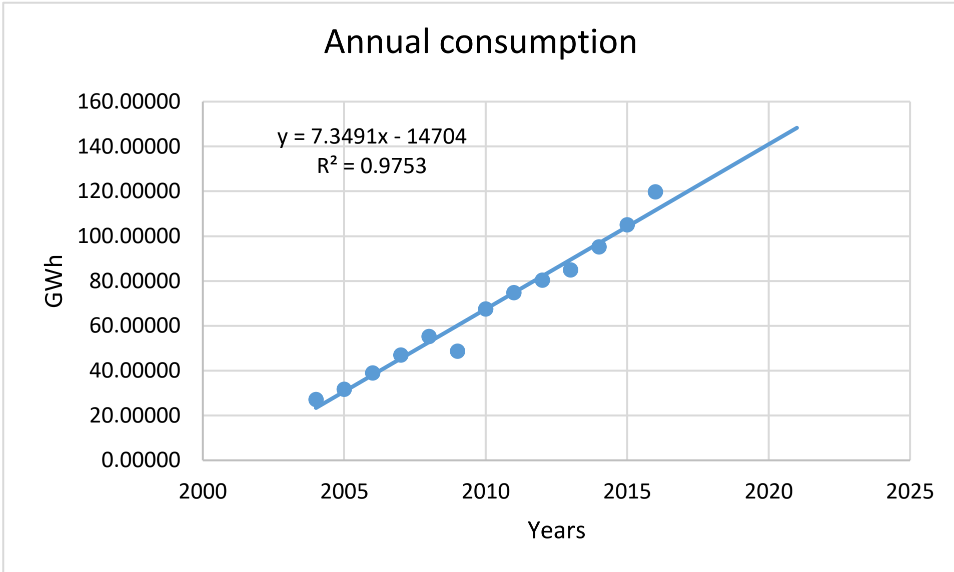

Fig.3.5 Annual consumption of the Tubas station load forecasting

By doing a linear curve of the annual load from 2004 to 2017, shows that the demand during 2020 is more than the capacity of the station through the following equation:

$$y = 7.3491x - 14704 \quad (3.1)$$

Where y and x are annual consumption and number of year respectively.

The previous data shows that the maximum load demand and maximum PV energy production occurs in July so we will take all the data during this month and the work of the average and insert the data on the ETAP software to make the analysis.

3.3 Description of PV Systems

In most developed cities PV flat-plate collectors are mostly used for solar generation but the power output can be fluctuations with a sudden (seconds time-scale) loss. PV generation penetration within residential and commercial feeders will negatively affect the network. Climate fluctuations such as clouds, cause large power fluctuations at the output of the PV solar facility due to the blocking of complete array strings if one module is shaded.

Recently a Tubas utility installed large 3 MW utility scale power, in addition to already installed 350 kW and 120 kW plants.

In Tubas areas cloud cover and fog may provide large power fluctuations with associated energy production loss, grid stability concerns, power quality, low capacity factors and power balancing problems. This thesis will study the effect of the three solar PV stations.

3.3.1 Maslamani PV Plant

Fig.3.6 represent largest PV plant (Masllamani Station) is located 9 km from the main station (Tayseer) in Faraa camp in the south of Tubas, with capacity of 3 megawatt (3MW), which is integrated to the main distribution network and started operating during late 2017. Fig.3.7 shows SLD of the Masllamani station in Tubas network.

Fig.3.6 Maslamani station

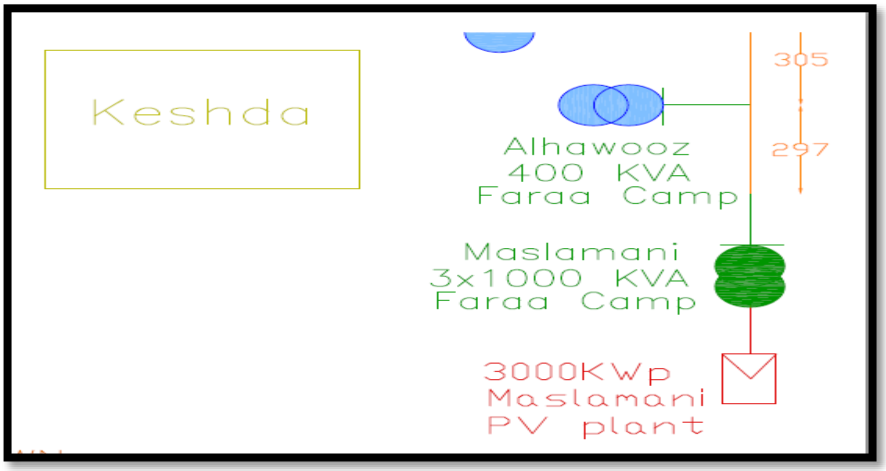

Fig.3.7 Maslamani integrated with Tubas network

Fig.3.8 SLD of the Maslamani station

Maslamani is divided to two station in the same place and connected on the grid by switchgear Table 3.2 shows the all specification of the Maslamani station.

Table 3.2 Specification of the Maslamani stations

	Station 1	**Station 2**
Power (kWp)	1878	1121
Power of panel (W)	320	320
# of panel	5871	3503
Power inverter (kVA)	60	60
# of inverter	31	19
# of string	302	190
# of panel per string	19	19

The name plat of the panel 320 Wpaxitecsolar manufactured in Germany as shown in Fig.3.9 and Fig.3.10 presently 60 kW SMA inverter as shown in Fig.3.9. The details of Maslmani components is shown in **appendix B**.

Fig.3.9 Panel characteristic

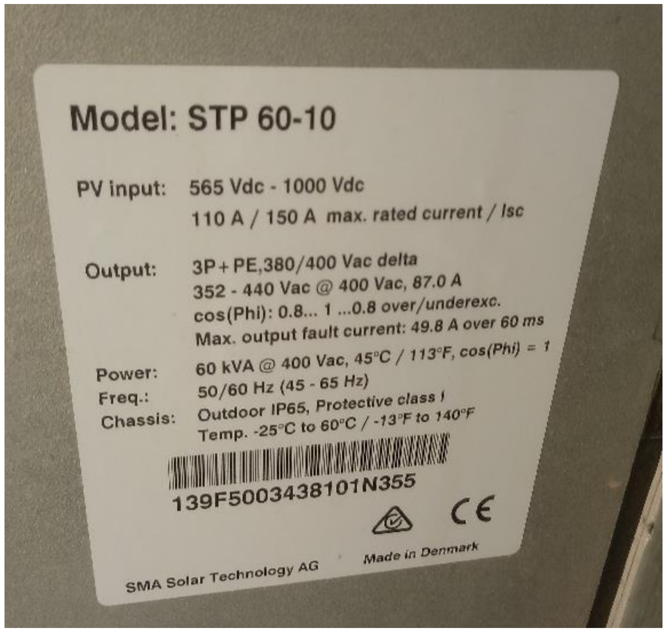

Fig.3.10 Inverter characteristic

Three 630 kVA,50Hz step-up transformers 0.4/33 kV connected with each other in parallel are connected with Tubas network.

By using PV-syst software for making analysis and optimization for solar stations, all parameters will be insert into the software as shown in Fig.3.11, the result is obtained in **appendix C**.

PV-syst analysis

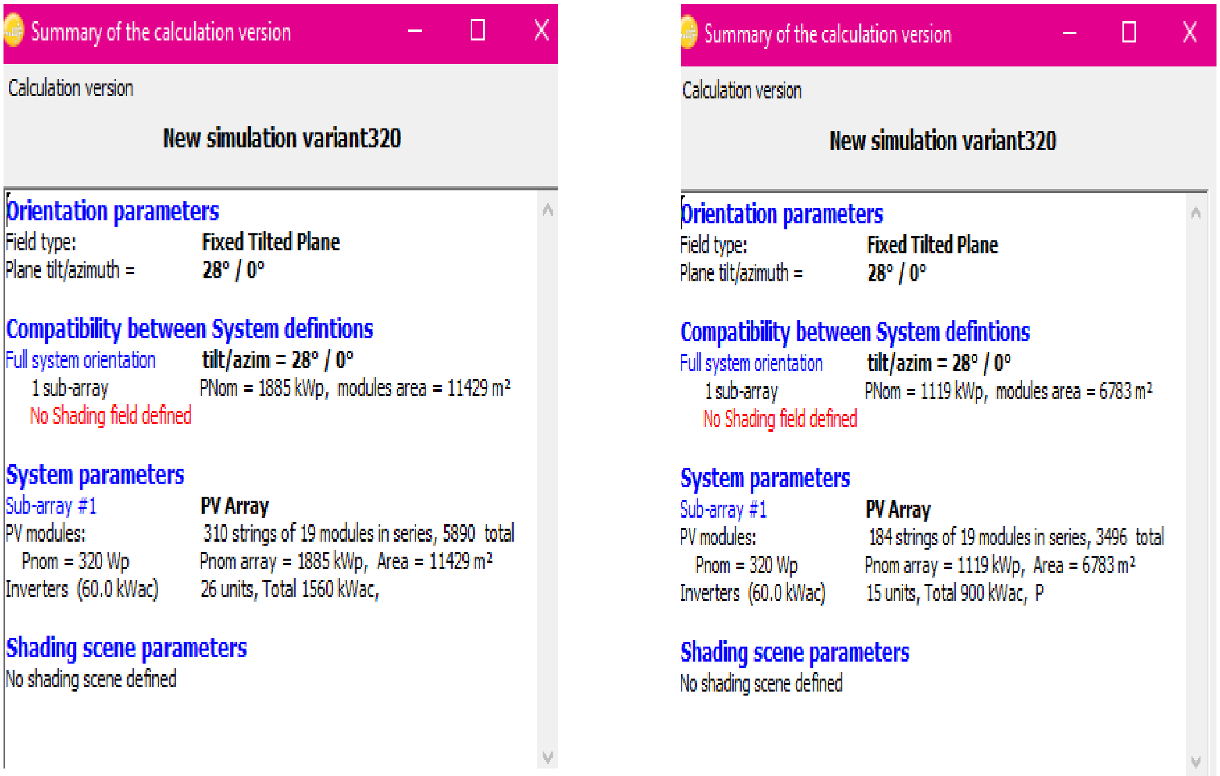

Fig.3.11 Information of the station from the PV-syst

3.3.2 Czechia Plant (350 and 120) kW

These stations are close to Musallmani station and we will study their impact on the network, The details of Czechia station component are shown in **appendix D**.

Table 3.3 Specification the Czechia stations

	Station 1	**Station 2**
Power (kWp)	350	120
Power of panel (W)	250	250
# of panel	1400	480
Power inverter (kVA)	30	30
# of inverter	12	4
# of string	302	190
# of panel for each string	19	19

By using PV-syst software for making analysis and optimization for solar stations, all parameters will be insert into the software as shown in Fig.3.12, the results are shown in **appendix E**

PV-syst analysis

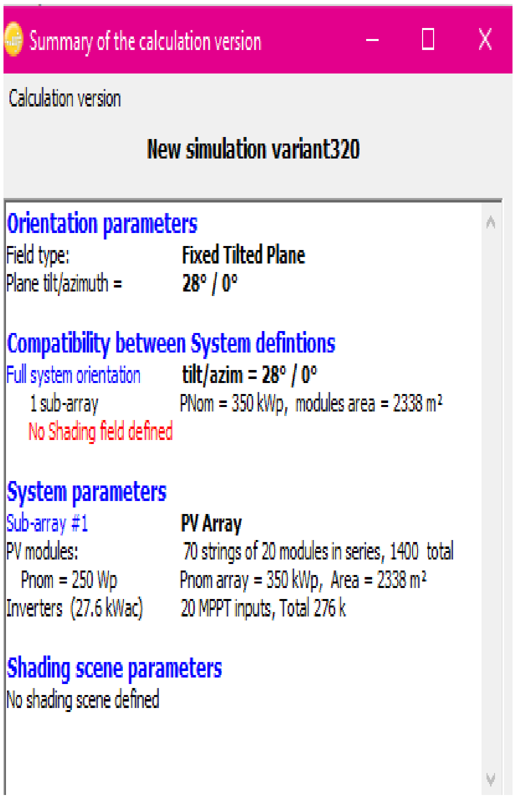

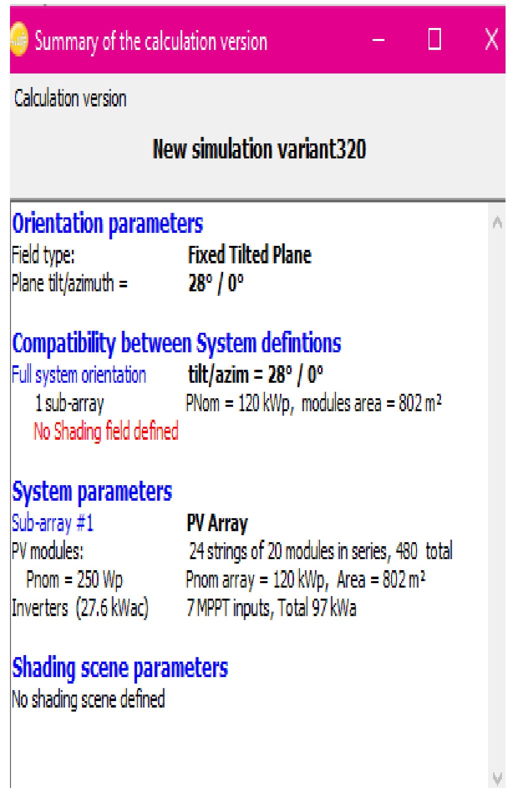

Fig.3.12 Information of the station from the PV-syst

4

Chapter 4: Simulation Results and Discussion

4.1 Introduction

In recent days, the using of software for analyzing the network with a numerical method became more commonly, because of its simplicity, the accuracy of measurements, the help it provides for planning and forecasting, and its ability to solve the problems. One of these software is Electrical Transient Analyzer Program (ETAP) which is the most comprehensive software used to design the integrated electrical systems, and which can provide many type of analysis such as the balanced load power flow unbalance load, in addition to being used to analyze power systems, faults, THD, short circuit analysis.

Modeling and simulation of a real power system network in Tubas was considered and a single line diagram is modeled using ETAP 16.0.0 software. All the physical and electrical parameters of the power system including height of towers, spacing between transmission lines, resistance and reactance values of transmission lines, transformer and generator ratings etc. are collected and coded to obtain the exact model of power system network. Then load flow study is conducted using the same software and simulation results are analyzed. Moreover From the results, the buses with low voltage profiles are identified and possible solutions for improving the voltages are studied and their effectiveness is checked using the software [21].
Integration of photovoltaic (PV) systems with high penetration level may introduce a many of adverse impacts on a grid operation. Voltage rise, reverse power flow and voltage unbalance can be listed as some of the major impacts.

In this chapter, the simulation of the electrical grid of Tubas will be analyzed in two periods of time, before and after connecting a PV plant to the network. The behavior with PV penetration is also essential for understanding these impact. A three-phase power flow approach is developed for the analysis of three phase plants solar PV impact of MV networks. To investigate the impacts of three-phase variable PV generation, a series of power flow calculations will be performed over a 24-hour period .A practical distribution system in tubas will be used to verify the applicability of the proposed approach in real-world distribution networks.

4.2 ETAP Design

Modelling has been performed using the ETAP simulation software based on the single-line diagram and the data of Tubas Substation Tayaseer Feeder. Load-flow analysis under steady-state condition has been done to simulate the condition before and after installing the PV power plants.

Load flow simulation has been undertaken by defining one bus as slack-bus with voltage of 1.0 p.u, while setting all buses to which the distributed plants have been connected with the voltage value of 1.0 p.u.

The complete test bus system has been first constructed in ETAP. Then a model of a typical solar PV plant is developed with the help of PV array block. Several such PV arrays have been created and pooled into a common 33kV bus solar bus. The output of the solar bus is then given to a station transformer which steps up the 400V generation voltage to 33kV, which would be suitable for penetration into transmission bus. Fig 4.1 shows single line diagram on 33kV network of a district inside composite network in ETAP software.

The design of the Tubas network contains a large number of load buses, but in this thesis the focus was on the buses starting from the main inter connection point to the PV buses and loads in between. The details of the distribution network are stated in **Appendix F.**

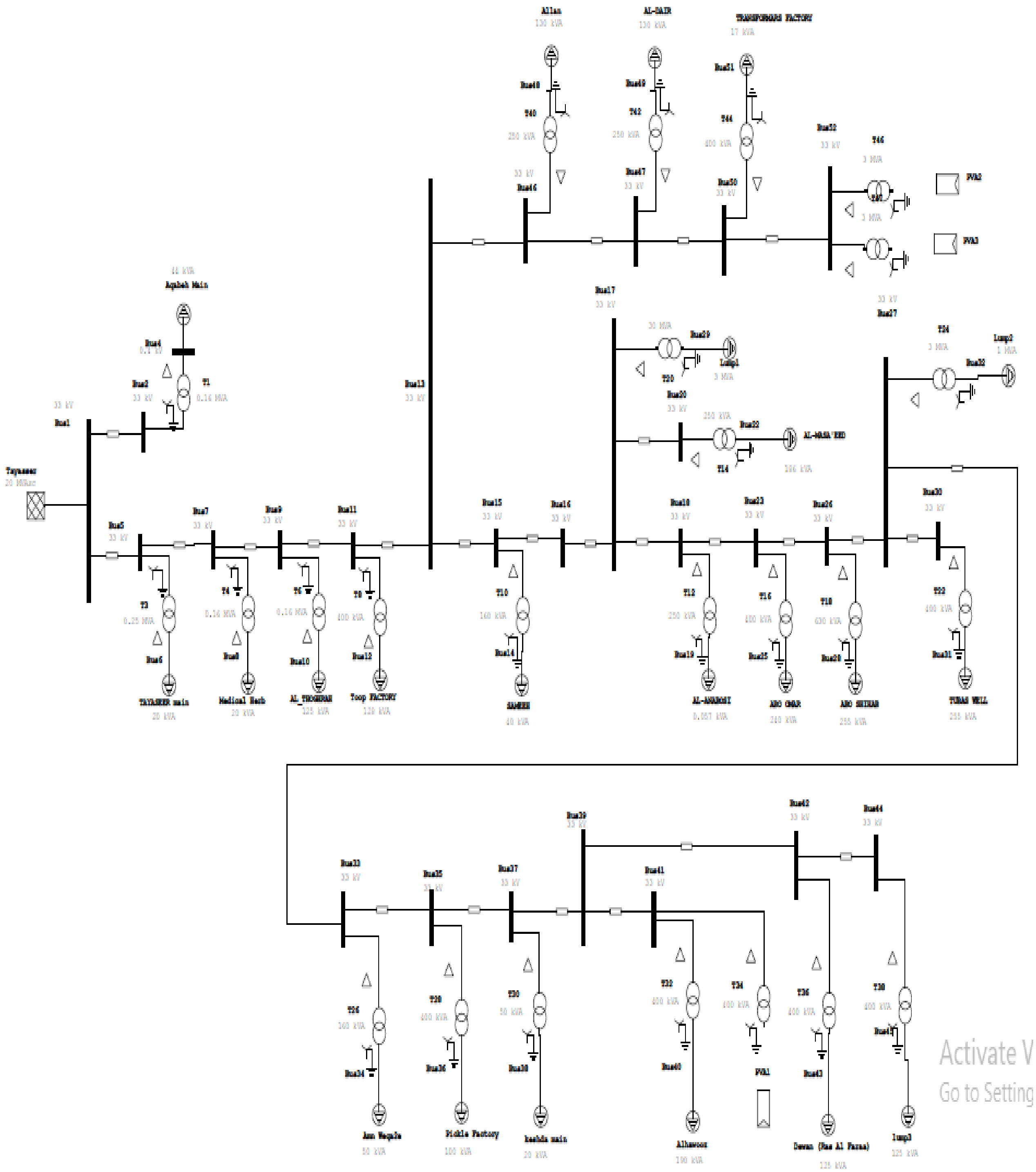

Fig.4.1The distribution network (33/0.4) kV of Tubas

4.2.1 Cables and Overhead Lines

Tubas network has a large number of cables and overhead with a different manufacturer and different size (50, 70,110,150) mm^2 which has an impedance value effect on the system. The cables in the network are very old and there is no data on them. The library at the software has the suitable and standard type of these conductors, so it's important to insert the resistance and reactance regarded to the length as it is written for each type in **Appendix F1** and all the data of distribution line analysis in ETAP.

Table 4.1 Standard cables and overhead lines

Data Line Type	**Resistance (Ω/km)**	**Reactance** (Ω/Km)	**Admittance (Ω^{-1} /km)**
Coyote	0.216	0.318	0
Dog	0.269	0.326	0
Rabbit	0.529	0.347	0
Nexans, single core XLPE, 95 mm2	0.321	0.22	$5.2*10^{-5}$

4.2.2 Transformers

The most important parameters should be taken into account to represent the transformers in ETAP software are the kVA rating, positive and negative impedances, and X/R ratio. Tubas network has a (50,160, 250, 400, 630) ratings with a different manufacturer, the parameter of X/R is attached in **Appendix F2** and all data of the transformer.

Table 4.2 Transformer data

Transformer rating (KVA)	**X/R**	**Z %**
50	1.5	4
160	1.5	4.5
250	2.5	4.3
400	4	4.7
630	6.3	4.49

Where X/R ratio of a transformer is simply the imaginary part of its impedance divided by the real part of its impedance, Z% percentage of the rated voltage applied to the transformer.

4.2.3 Loads

In ETAP software there are lumped load that is used for unbalanced load analysis and static load that helps to analyze the harmonics. In this thesis, an application of the consumer will be done. However, to use lumped load to design an electrical system the average power for three phases should be estimated according the data from the TEDCO to ensure the accuracy results.

4.3 ETAP Results

The connection of the DG on the electrical network has direct impact on the operation and performance of the network, there are some changes to the characteristics of the network such as the voltage profile, harmonic and the power factor. The output result from the ETAP in **Appendix F3.**

4.3.1 Voltage Unbalance

The literature indicates clearly that integrated DG could impact the voltage of the distribution grid [26]. From the selected feeder, the voltage measured at the substation end is unstable even in the condition where the whole feeder was supported by PV generation as described above. The fluctuation range is ±7%, as shown in Fig.4.2.

The production of solar energy shall be as high as possible in the middle of the day, depending on climatic conditions and temperature. Household load demand is comparatively high during this time, and power generation from PV sources is high too. Therefore it may exceed the load level at the PV connection point at this time, and voltage rise may be observed. There are two locations collect the data required which are Tayasser and AL-Fara as shown in Fig.4.2 and Fig.4.3 respectively.

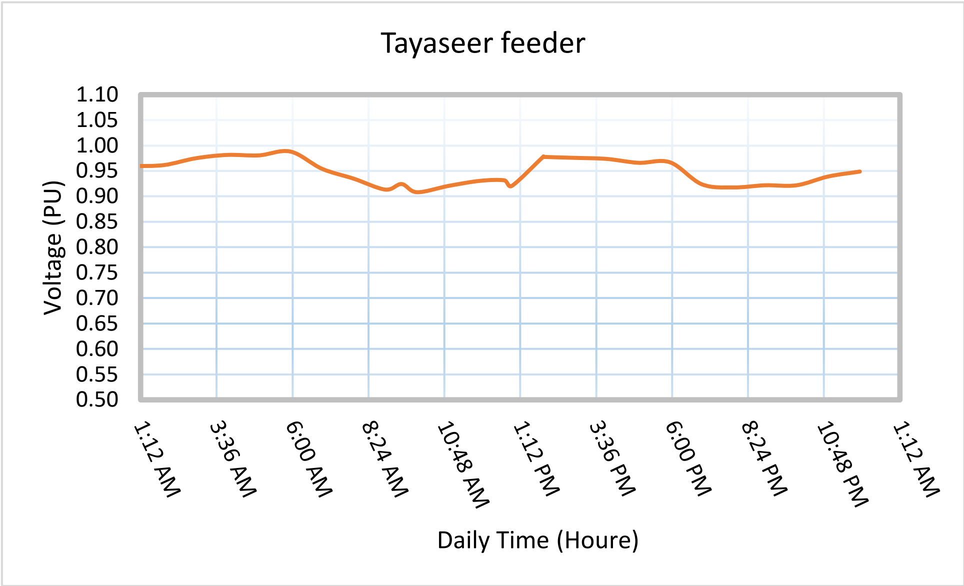

Fig.4.2 Feeder voltage profile (Tayasser)

It is clear from the Fig 4.2 that the voltage at the feeder is unbalanced and this is a big problem. The reading of the voltage at AL-Fara at the same time has voltage drop because of the load assumption as shown in Fig.4.3.

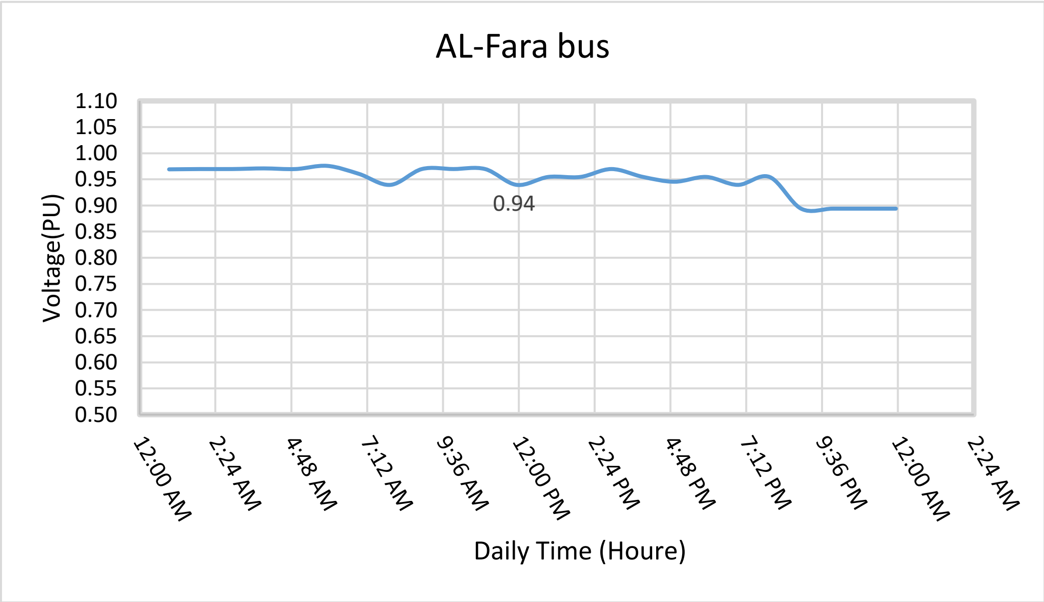

Fig.4.3 AL-Fara voltage profile

After analyzing Al-Fara metering at bus 27 (AW). By comparing the results to the fara bus between real and simulation were the same value.

The DG produces more power than the local demand. The net power will flow upstream (towards the substation). If this reverse power flow is sufficiently large, it will overcome the voltage drop caused by the reactive power flow and may result in an over voltage at the energy connection point (ECP) [27].Through the simulation of the ETAP software it was found the voltage drop at each bus at maximum PV production and maximum load with and without PV, as shown in Fig.4.4

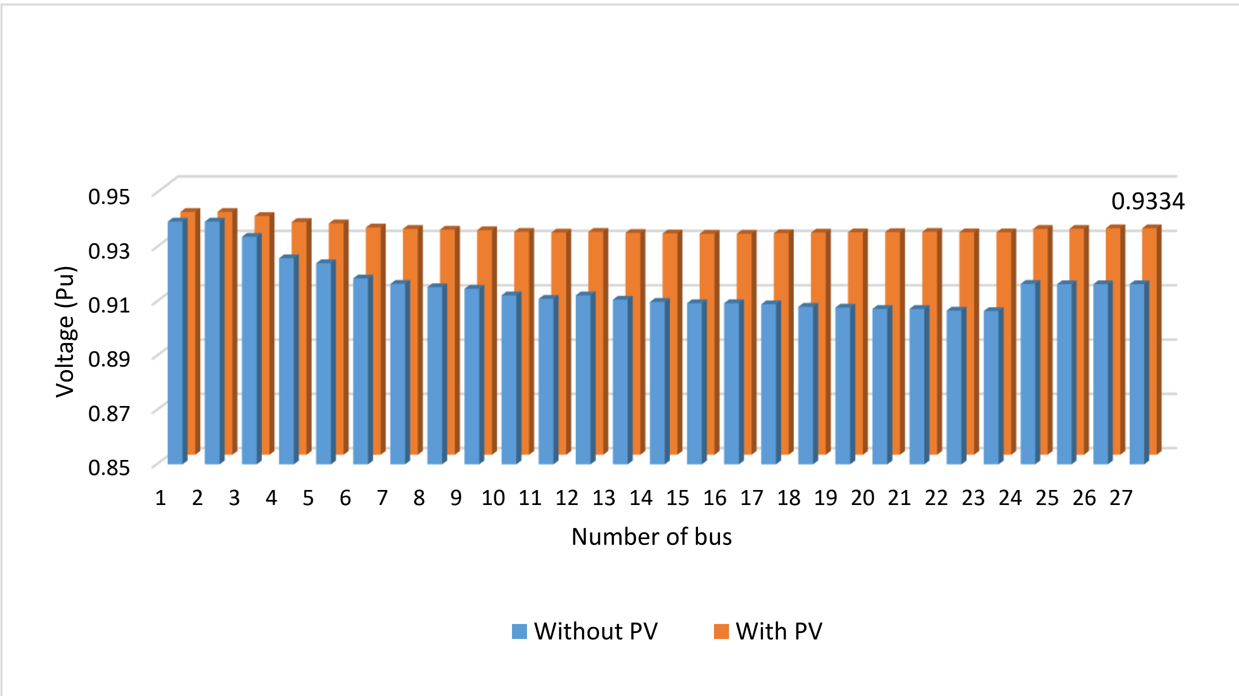

Fig.4.4 Variation in voltage at different buses with and without solar PV

The branch current at MV will decrease because the PV plant supplied the near load from the power which leads to decrease the branch current load as shown in Fig.4.5.

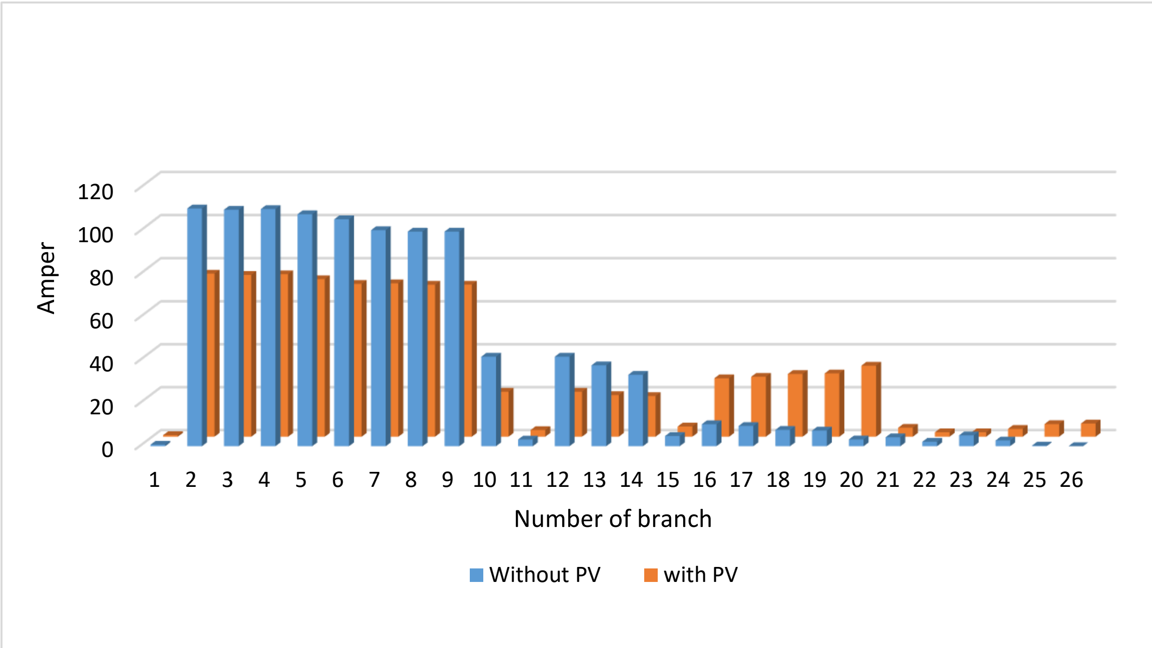

Fig 4.5 Variation in branch current loading with and without solar PV integration.

4.3.2 Active and Reactive Power

The load profile of the grid in the last years was very high, the value of 20MVA installed will be reached in some time, even in the months of more activity. The demand of power monitored in both periods (2004 to 2017) reach 80 percent from the rated, Fig.4.5 represent annual consumption of the Tubas area. And on the other hand after running the PV plants at end of 2017 produced 3,470 MW in optimal conditions, so the reverse power flow could be.

The PV inverters are subject to the action of control systems aimed at providing zero reactive power at fundamental frequency, but several experiences have shown that the filters of inverters are not disconnected consuming reactive power, even when PV plant is not operating. This fact does not justify such a reactive power consumption, which may be due to increased loads on the grid in recent years.

4.3.3 **Power Factor**

The PV inverters are operated at unity power factor as can be observed in Fig.4.6 the power factor decreases to unacceptable levels during PV system operation this figure represents the power factor at Tayasser within one day in July. When PV system works with high power values closes to rated ones, most active power demanded by the customers is supplied by the PV plant, reducing the demand of active power from the grid. However reactive power demand is the same, so it causes a low power factor measured at the substation represented in table 4.3 in more than one cases.

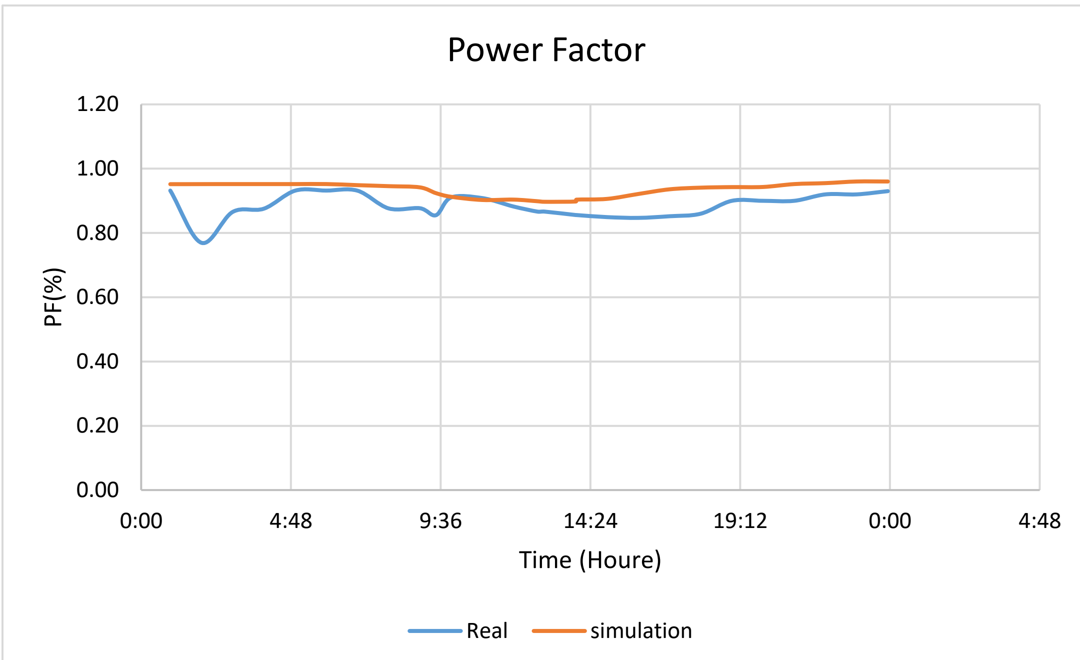

Fig 4.6 Measurements at the substation in 24 hours recording the power factor with PV

Table 4.3 Power factor of the substation

Case	**Power factor**
Without PV	93.88
With PV 50% Production	92.91
With PV full Production	91.27

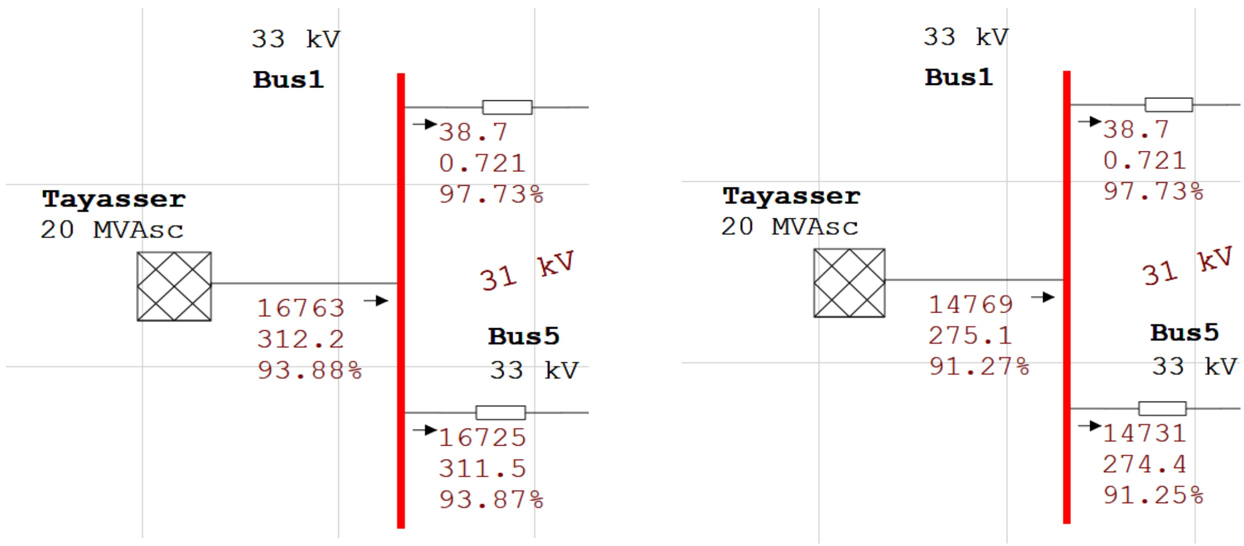

Fig.4.7 Power grid represented by ETAP a) without PV b) with PV

From the Fig.4.7 nots that the PV production decrees the power factor and the bus red line this means that the voltage critical point (undervolted) which causes islanding at the PV inverter.

4.3.4 Power Losses

Steady-state power flow analysis is used to examine the power losses variation for a variety of distributed generation penetration. Based on the power flow analysis, power losses due to the power plants injection can be determined. Three different scenarios are determine the effect of dispersed generation injection are proposed. Starting from the original grid in the first scenario without connected PV plant, and being added with photovoltaic plants half production in the second scenario, the last scenario with full production PV plants. The considered scenarios are based on the existing potential of the plants in the network system under concern.

From the point of view of power loss analysis, Scenario 3 also results in the smallest loss compared to the other scenarios. The least favorable losses reduction is given by Scenario 3 using the wind power plant injection, despite that the injection of renewable energy power plants in this study in general is proven to improve the voltage profile and reduction of power losses in the system.

Fig.4.8 represent three scenario to measure the power losses and shows the efeect on the power losses.

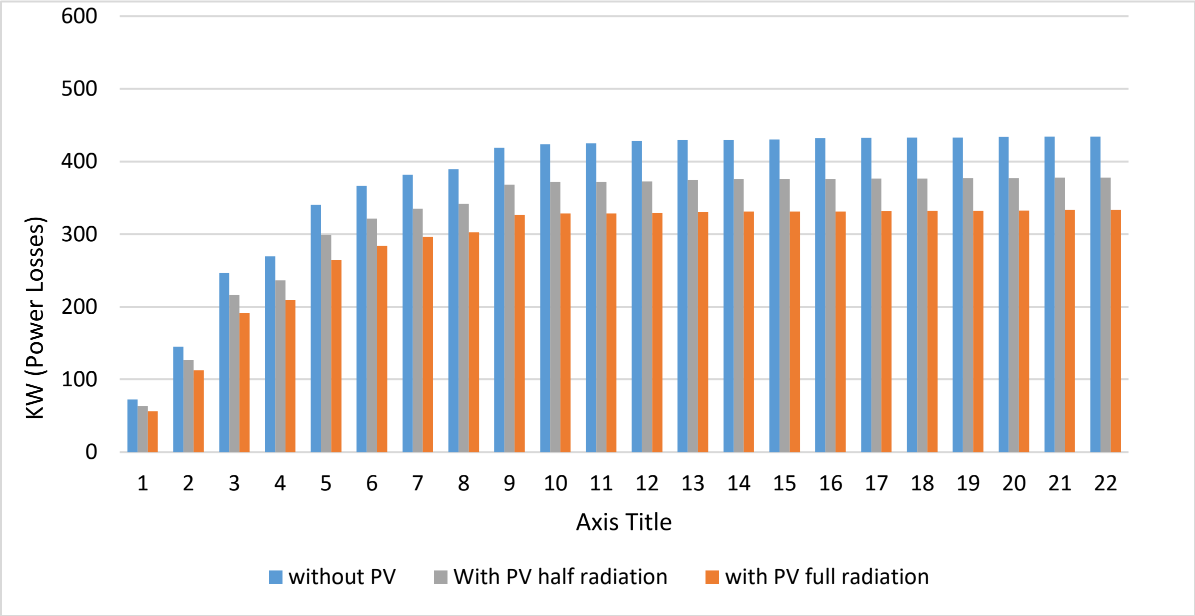

Fig.4.8 Power losses representing the three scenarios

5

Chapter 5: Enhancement of Performance of Tubas Network Based on Simulation

5.1 Introduction

Solar photovoltaic (PV) resources are the most commonly observed form of distribution generation (DG at the residential customer premises in low voltage (LV) distribution networks. Depending on their capacity, the solar PV units serve part of the loads locally that reduces the stress on the distribution feeder and improve system performance by reducing feeder loss and releasing system capacity. However, a high penetration level of PV resources can impose several challenges for distribution network operators, such as, reverse power flow and voltage rise problem at MV networks.

If the PV generation is greater than the local demand at the point of common coupling (PCC), the excess power from PV inverters may produce reverse power flow in the feeder that would create voltage rise. With a high penetration of stations PV resources at MV level, there is a possibility of the upper limit violation. But the voltage at Tayaseer feeder is less than 95 % p.u voltage some time causes islanding on the PV inverter, a solution is required to reduce the overvoltage problem caused by the PV solar station.

This chapter, propose two scenarios of development and improvement for Tubas distribution network. The proposed strategy is more advantageous for PV impact mitigation and evening load support. The first one add Tap changer transformer at the feeder Tayasser to save voltage input constant (33kV). The second one will be add new feeder to minimize the voltage drop from the load that causes islanding and convert the network from radial to ring.

5.2 TAP Changer Transformer Solution

Generally the load on the feeders varies, the voltage drop between the substation (beginning of the feeder) and the end user will vary. For maintaining the voltage at the users within an acceptable range and to avoiding islanding of the PV inverters voltage regulators were proposed to add to the system. On loads TAP changers selected to maintain the voltage of the feeders are within plus or minus 3%.

TAP changer approach are installed at the Tayaseer transformer on ETAP simulation software as shown in Fig.5.1,and the result shows that the voltage drop at the consumer part is still within acceptable range as shown in Fig.5.2.

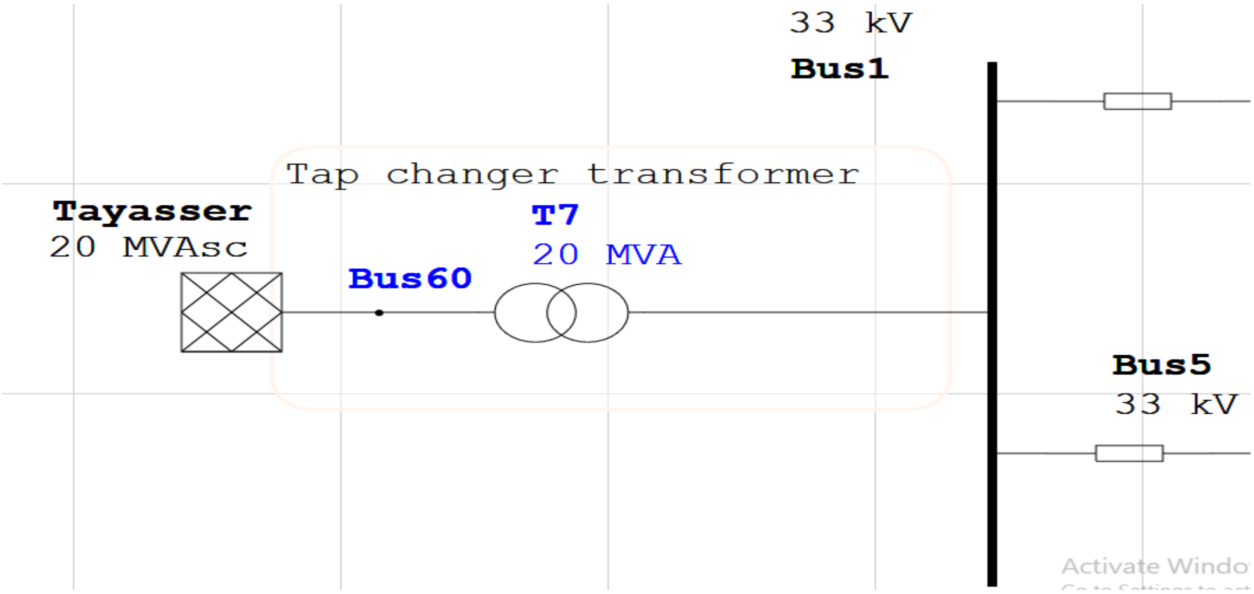

Fig.5.1 Tap changer transformer in ETAP software

5.2.1 Voltage Effect

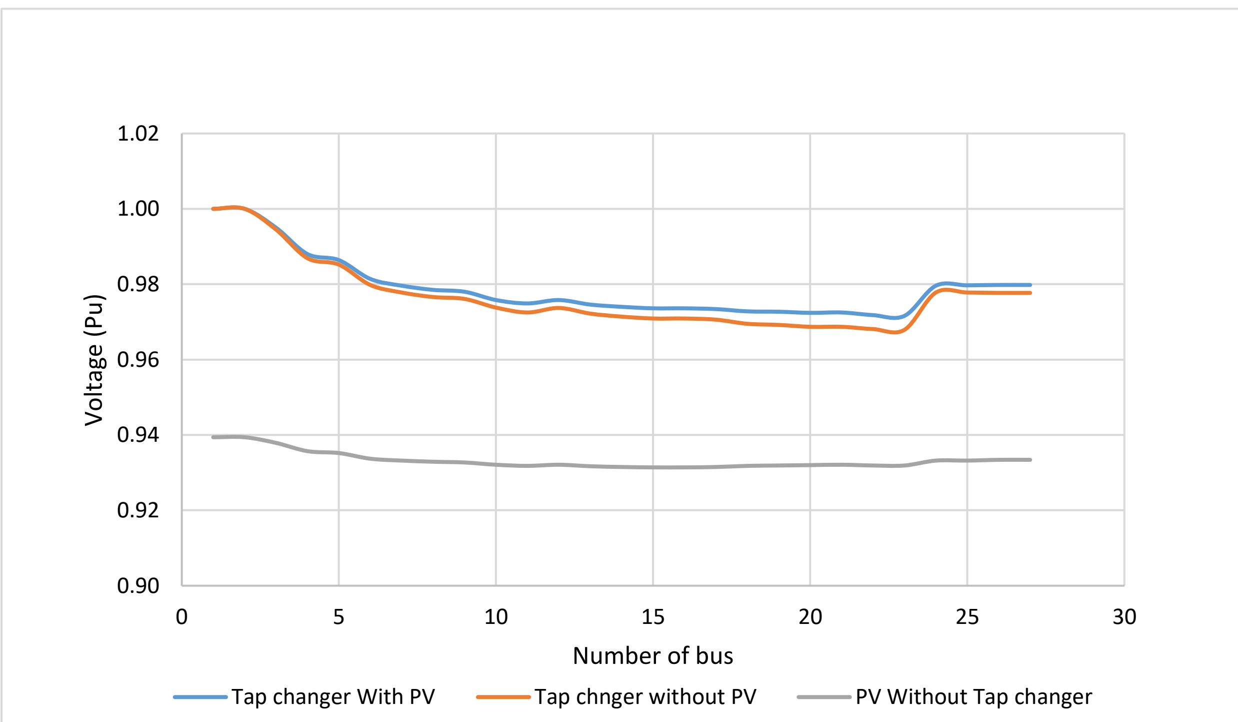

Fig.5.2 Effect of the Tap changer on the MV network

5.2.2 Power Losses Effect

After the voltage is balanced, the average power losses is reduced by 14 %. This due to in reducing the load at the main inter connection point "Tayasser" as shown in Fig.5.3.

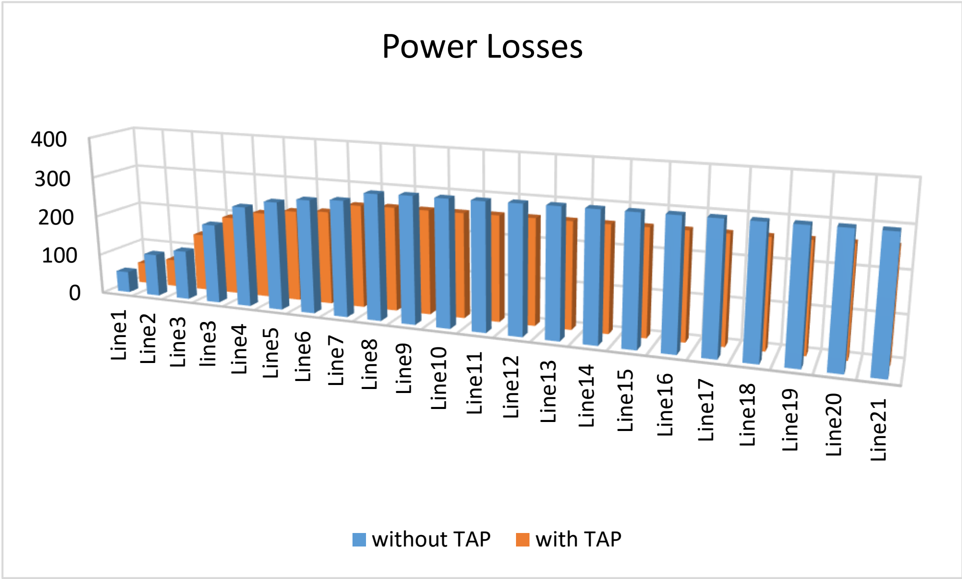

Fig.5.3 Power losses affected by the Tap changer

5.3 New Inter-Connection Point Solution

Tubas grid is a radial distribution network. However the main drawback of radial electrical power distribution system can be overcome by introducing a ring main electrical power distribution system. Here one ring network of distributors is fed by more than one feeder. In this case if one feeder is under fault or maintenance, the ring distributor is still energized by other feeders connected to it. In this way the supply to the consumers is not affected even when any feeder becomes out of service.

In addition to that the second inter connection point will reduced the distance between the substation and the load which decrees the voltage drop and the power losses on the feeder, not to mention increasing the possibility the continuity of the system, if any fault occurs on any section, of the ring, this section can easily be isolated by opening the associated section isolators on both sides of the faulty zone transformer directly Total Length of the Ring is Main Distributor. It is long enough. To compensate the voltage drop in the line, more one feeder to be connected to the ring system.

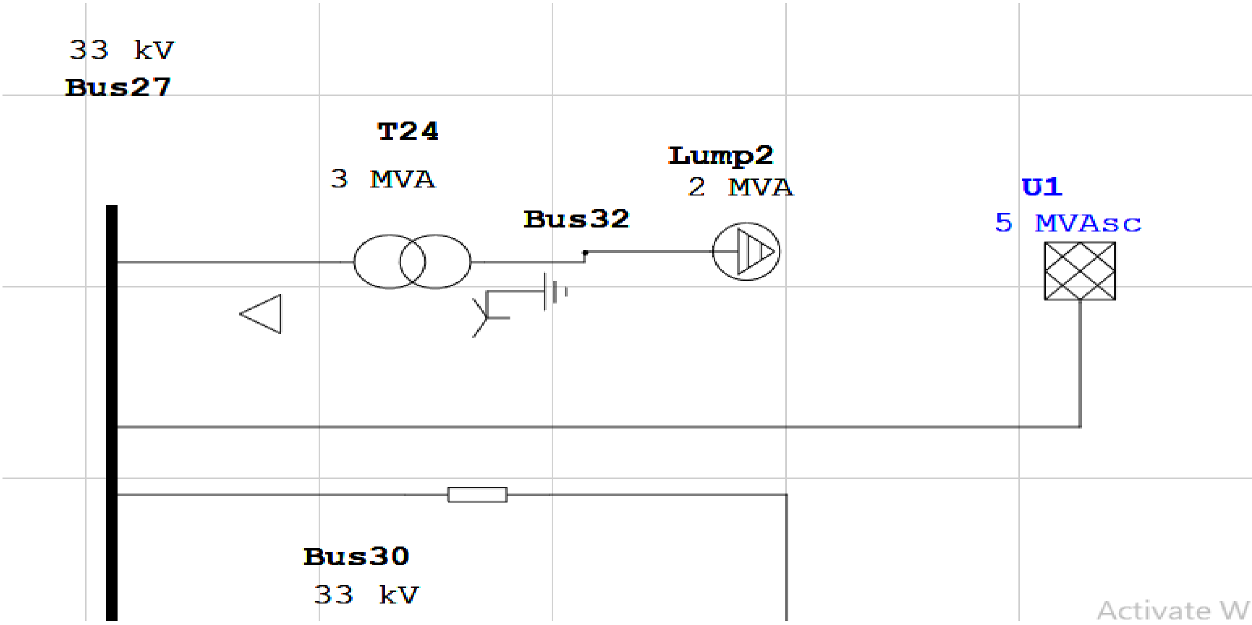

Fig.5.4 New feeder added to network represented by SLD

Comparison analysis between the current and the suggested location of the new feeder:

5.3.1 Voltage Effect

After adding the new feeder, the voltage drop reached 6%. As shown in Fig.5.5.

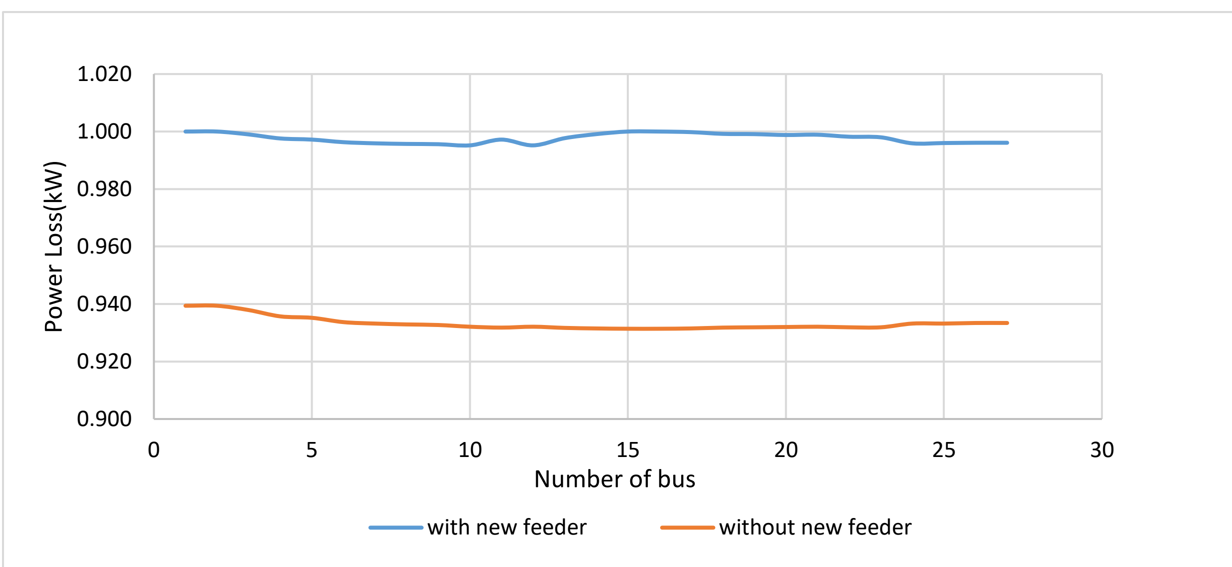

Fig.5.5 The effect of adding feeder on the MV

5.3.2 Power Losses Effect

After adding the new feeder was balanced, the average power losses was reduced by 5 %. as shown in Fig.5.6

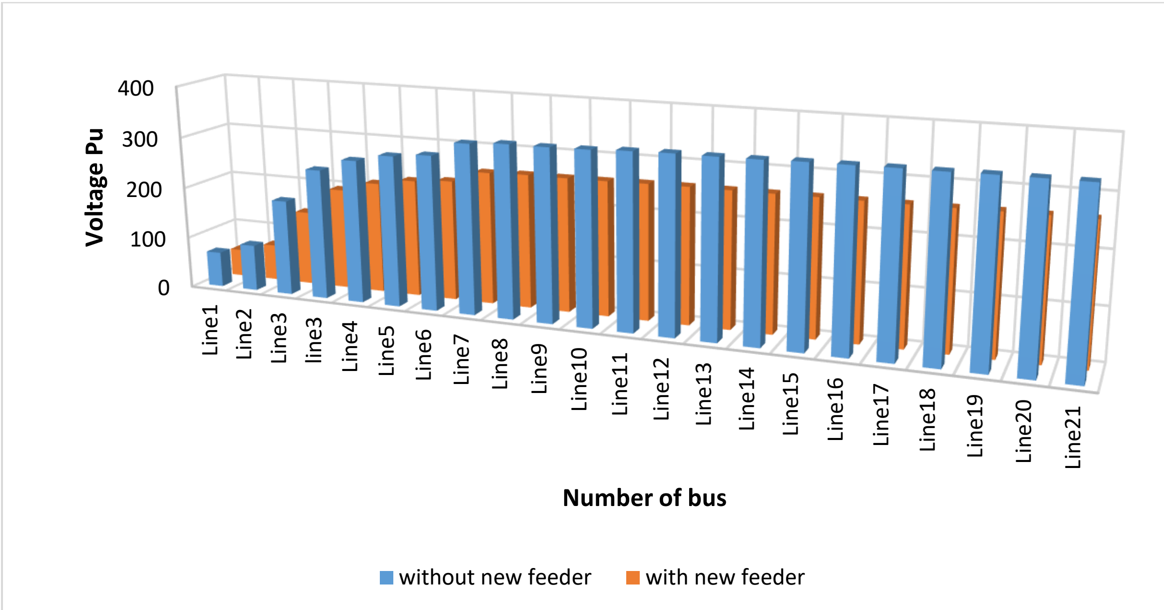

Fig.5.6 Power losses affected from add new feeder

5.4 Conclusion

Load-flow studies are important for planning future expansion of power systems as well as in determining the best operation of existing systems. Solar energy production reduces losses on grid lines because the amount of consumption of the main feeder decreases. When the sunlight is blocked by clouds or shading from surroundings, the power from the PV system can be dropped sharply. Renewable energy resources when implemented in large scale without any specialized control is found to impact the integrity, reliability, security and stability of the power grid. Tubas station suffers from many problems in the network as the analysis shows. In this thesis, the voltage on the main feeder is unbalanced and drop to 0.85 Pu and the power losses will increase since the network is a ring network. Tubas region suffers from electric flickers due to low voltage and high loads at one point. All Tubas region previously-mentioned problems exist due to the existence of large solar power stations will the network is not prepared or qualified to receive the output of these plants. For this reason, the case must be well studied and solutions should be proposed to these problems found.

The proposed strategy to mitigate the network by adding Tap changer transformer at the feeder Tayasser to keep voltage input constant (33kV). The second one will be add new feeder to change the network from radial to ring. When the tab changer transformer was added to the main feeder, the voltage at the buses dropped to 3% compared to the network without tab changer. Consequently, the power losses were reduced by 14% as well. And when a new feeder was proposed, the power consuming from the Taysser was reduced and then the power losses drop all the way to reach to 5%.

The information obtained using the proposed approach would be beneficial to implement mitigation actions against adverse impacts of PV penetration including fluctuations caused by sudden variations in PV output.

5.5 Recommendation

1- For Tubas Electricity

- Connect smart meters to all distribution transformers in order to monitor and manage loads.
- Workshop on the utility of improving the power factor of the consumer.
- The importance and necessity of connecting the ring system for 33KV network.

2- For our University

- The need for power network simulation programs with all license.
- Add new courses for teaching the student how to use ETAP and other simulations software's.

5.6 Future Work

Research in a more accurate restrain region is required for diverse distributed renewable generation. To stabilize the voltage dynamically, a corresponding algorithm is also needed to control sinking or sourcing reactive power from or to the grid. For future smart micro-grid and smart grid operation, an economical and reliable storage system.

PV generation is a fairly mature renewable generation technologies but has much opportunity to improve in efficiencies and cost reduction.

Be able to use light, which was first created by God, to not only brighten our lives, but to power our future.

References

[1] P. González, E. Romero-Cadaval, E. González, and M. A. Guerrero, “Impact of grid connected photovoltaic system in the power quality of a distribution network,” in *Doctoral Conference on Computing, Electrical and Industrial Systems*, 2011, pp. 466–473.

[2] F. Katiraei, K. Mauch, and L. Dignard-Bailey, “Integration of photovoltaic power systems in high-penetration clusters for distribution networks and mini-grids,” *Int. J. Distrib. Energy Resour.*, vol. 3, no. 3, pp. 207–223, 2007.

[3] R. A. Walling, R. Saint, R. C. Dugan, J. Burke, and L. A. Kojovic, “Summary of distributed resources impact on power delivery systems,” *IEEE Trans. power Deliv.*, vol. 23, no. 3, pp. 1636–1644, 2008.

[4] M. Thomson and D. G. Infield, “Network power-flow analysis for a high penetration of distributed generation,” *IEEE Trans. Power Syst.*, vol. 22, no. 3, pp. 1157–1162, 2007.

[5] A. Canova, L. Giaccone, F. Spertino, and M. Tartaglia, “Electrical impact of photovoltaic plant in distributed network,” *IEEE Trans. Ind. Appl.*, vol. 45, no. 1, pp. 341–347, 2009.

[6] K. Jadeja, “Major technical issues with increased PV penetration on the existing electrical grid.” Murdoch University, 2012.

[7] J. H. R. Enslin and H. Alatrash, “Distribution Network Impacts of High Penetration of Distributed Photovoltaic Systems,” in *21 International Conference on Electricity Distribution, Frankfurt, 6-9 June 2011*, 2011.

[8] M. Karimi, H. Mokhlis, K. Naidu, S. Uddin, and A. H. A. Bakar, “Photovoltaic penetration issues and impacts in distribution network–A review,” *Renew. Sustain. Energy Rev.*, vol. 53, pp. 594–605, 2016.

[9] K. L. Butler-Purry and M. Marotti, “Impact of distributed generators on protective devices in radial distribution systems,” in *Transmission and Distribution Conference and Exhibition, 2005/2006 IEEE PES*, 2006, pp. 87–88.

[10] S. Conti, S. Raiti, G. Tina, and U. Vagliasindi, “Study of the impact of PV generation on voltage profile in LV distribution networks,” in *Power Tech Proceedings, 2001 IEEE Porto*, 2001, vol. 4, p. 6–pp.

[11] A. Kumar, M. P. Selvan, and K. Rajapandiyan, “Grid Stability Analysis for High Penetration Solar Photovoltaics.”

[12] R. Albarracín and H. Amarís Duarte, “Power quality in distribution power networks with photovoltaic energy sources,” 2009.

[13] E. Demirok, D. Sera, R. Teodorescu, P. Rodriguez, and U. Borup, “Clustered PV inverters in LV networks: An overview of impacts and comparison of voltage control strategies,” in *Electrical Power & Energy Conference (EPEC), 2009 IEEE*, 2009, pp. 1–6.

[14] C. L. T. Borges and D. M. Falcao, “Optimal distributed generation allocation for reliability, losses, and voltage improvement,” *Int. J. Electr. Power Energy Syst.*, vol. 28, no. 6, pp. 413–420, 2006.

[15] T. E. Kim and J. E. Kim, “A method for determining the introduction limit of distributed generation system in distribution system,” in *Power Engineering Society Summer Meeting, 2001*, 2001, vol. 1, pp. 456–461.

[16] A. Hasibuan, S. Masri, and W. Othman, “Effect of distributed generation installation on power loss using genetic algorithm method,” in *IOP Conference Series: Materials Science and Engineering*, 2018, vol. 308, no. 1, p. 12034.

[17] M. Tonso, J. Moren, S. W. H. de Haan, and J. A. Ferreira, “Variable inductor for voltage control in distribution networks,” in *Power Electronics and Applications, 2005 European Conference on*, 2005, p. 10–pp.

[18] B.-I. Crăciun, T. Kerekes, D. Séra, and R. Teodorescu, “Overview of recent grid codes for PV power integration,” in *Optimization of Electrical and Electronic Equipment (OPTIM), 2012 13th International Conference on*, 2012, pp. 959–965.

[19] J. R. Abbad, “Electricity market participation of wind farms: the success story of the Spanish pragmatism,” *Energy Policy*, vol. 38, no. 7, pp. 3174–3179, 2010.

[20] A. Fediaevsky, J.-J. Bénet, M. L. Boschiroli, J. Rivière, and J. Hars, "La tuberculose bovine en France en 2011, poursuite de la réduction du nombre de foyers," *ANSES Bull Epidemiol*, vol. 54, pp. 4–12, 2011.

[21] V. Raveendran and S. Tomar, "Modeling, Simulation, Analysis and Optimisation of a Power System Network-Case Study," *Int. J. Sci. Eng. Res.*, vol. 3, no. 6, 2012.

[22] M. G. Villalva, J. R. Gazoli, and E. Ruppert Filho, "Modeling and circuit-based simulation of photovoltaic arrays," in *2009 Brazilian Power Electronics Conference*, 2009, pp. 1244–1254.

[23] M. R. Patel, *Wind and solar power systems: design, analysis, and operation*. CRC press, 2005.

[24] M. M. El-Saadawi, A. E. Hassan, K. M. Abo-Al-Ez, and M. S. Kandil, "A proposed framework for dynamic modelling of photovoltaic systems for DG applications," *Int. J. Ambient Energy*, vol. 32, no. 1, pp. 2–17, 2011.

[25] M. M. El-Saadawi, A. E. Hassan, K. M. Abo-Al-Ez, and M. S. Kandil, "A proposed dynamic model of Photovoltaic-DG system," in *2010 1st International Nuclear & Renewable Energy Conference (INREC)*, 2010, pp. 1–6.

[26] P. P. Barker and R. W. De Mello, "Determining the impact of distributed generation on power systems. I. Radial distribution systems," in *2000 Power Engineering Society Summer Meeting (Cat. No. 00CH37134)*, 2000, vol. 3, pp. 1645–1656.

[27] M. Shen, "Distributed Solar Photovoltaic Grid Integration System: A Case Study for Performance," 2012.

[28] PV-syst software, PV-syst 6.3.8 , 2015.

APPENDICES

Appendix A: Single line diagram of the Tubas

Appendix B: Maslamni component

SEM TRANSFORMATÖR	**Technical Specifications**	Doc.No:	PF.13.04
		Publishing Date:	14.07.2014
		Revision:	00
		Date:	**13.01.2017**

1.	Manufacturing Standards		IEC 60076-1
2.	Product Type		Transformer with Conservator
3.	Service Type/ Cooling Method		Continuous Service / ONAN
4.	Rated Power	kVA	630
5.	Rated Voltages	HV / LV (kV)	33 / 0.4
6.	Tapping Range & No of Taps (HV, Off-Load Tap Changer)		5 taps ±2 x 2.50%
7.	Number of phases		3
8.	Frequency	Hz	50
9.	Connection Group		Dd
10.	No- Load Losses	W	899
11.	Load Losses	W	5100
12.	Impedance Voltages (at 75 °C and nom. pos.)	%	4 ± 10%
13.	No- Load Current	%	1.6 + %30
14.	Max. Ambient Temperature	°C	55
15.	Temperature Rise i)Windings ii)Oil	 K K	 50 45
16.	Core Type		Core - Cold Rolled Grain Oriented
17.	HV and LV windings		Electrolytic Copper
18.	Tank cover		Bolted
19.	Transformer Dimensions i)Width ii)Length iii)Height	 mm mm mm	 950 1798 2020
20.	Transformer Weights i) Total Weight ii) Oil Weight iii) Active Part Weight	 kg kg kg	 2100 430 1470
21.	Short- Circuit Withstand Duration	s	2
22.	Insulation Levels i)One Minute Power Frequency Withstand Voltage ii)Lightning Impulse Withstand Voltage		HV(kV) LV(kV) 70 3 170 -
23.	Insulation Class		Class A

Notes

Losses are according to IEC tolerances (Po + 15%,Pk + 15%,Ptot +10%).
Dimensions and weights are approximate.
First filling of mineral oil as per IEC 60296.
Painting is according to manufacturer standards (without galvanizing End color: RAL 7033).
Bushings are porcelain type.

Accessories :
Wheels, Oil Level Indicator, Thermometer Pocket, Dehydrating Breather, Earth Screen between HV and LV

ACSR

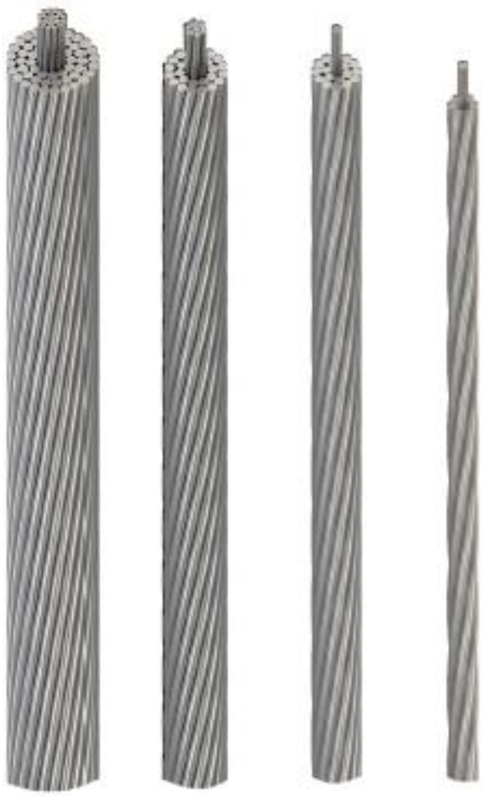

TEKNİK BİLGİLER

Orta ve yüksek gerilim iletim hatlarında kullanılırlar. TS EN 50182 Standardına uygun olarak alüminyum tellerden ve çinko kaplı çelik tellerden imal edilirler. İletkenler yedi veya daha fazla tellerden eş merkez tabakalı olarak örülürler. Eğer iletken birden fazla tabakadan oluşuyorsa bitişik tabakalar birbirine ters adım yönünde örülür. İstenildiğinde DIN, BS, ASTM, NF, CSA, EN standartlarına uygun üretim yapılabilir.

TECHNICAL DATA

They are used in medium and high voltage transmission lines. The aluminium wires and zinc coated steel wires are produced in accordance with TS EN 50182 standards. Conductors are stranded with seven or more wire as concentrically.If conductors are consist of more than one layer, than they are stranded in reverse direction to each other. Upon request they can be produced in accordance to DIN,BS, ASTM, NF, CSA, EN standards..

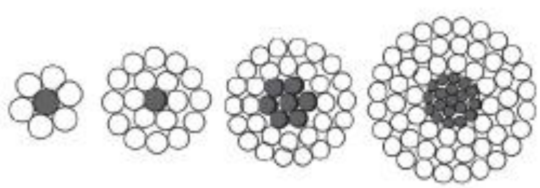

6 Al./1 St. 18 Al./1 St. 26 Al./7 St. 54 Al./19 St.

PVSYST V6,78		04/02/19	Page 1/1

Characteristics of a PV module

Manufacturer, model :	**Axitec Energy, AXIpower AC-320P/72S**
Availability :	Prod. Since 2015
Data source :	Manufacturer 2018

STC power (manufacturer)	**Pnom**	**320**	**Wp**	**Technology**		**Si-poly**	
Module size (W x L)		0,992 x 1,956	m²	Rough module area	Amodule	1,94	m²
Number of cells		1 x 72		Sensitive area (cells)	Acells	1,75	m²

Specifications for the model (manufacturer or measurement data)

Reference temperature	TRef	25	°C	Reference irradiance	GRef	1000	W/m²
Open circuit voltage	Voc	45,8	V	Short-circuit current	Isc	9,03	A
Max. power point voltage	Vmpp	37,6	V	Max. power point current	Impp	8,52	A
=> maximum power	Pmpp	320,0	W	Isc temperature coefficient	muIsc	3,6	mA/°C

One-diode model parameters

Shunt resistance	Rshunt	350	ohm	Diode saturation current	IoRef	0,028	nA
Serie resistance	Rserie	0,34	ohm	Voc temp. coefficient	MuVoc	-149	mV/°C
				Diode quality factor	Gamma	0,94	
Specified Pmax temper. coeff.	muPMaxR	-0,40	%/°C	Diode factor temper. coeff.	muGamma	0,000	1/°C

Reverse Bias Parameters, for use in behaviour of PV arrays under partial shadings or mismatch

Reverse characteristics (dark)	BRev	3,20	mA/V²	(quadratic factor (per cell))	
Number of by-pass diodes per module		3		Direct voltage of by-pass diodes	-0,7 V

Model results for standard conditions (STC: T=25°C, G=1000 W/m², AM=1.5)

Max. power point voltage	Vmpp	37,5	V	Max. power point current	Impp	8,52	A
Maximum power	Pmpp	320,0	Wc	Power temper. coefficient	muPmpp	-0,39	%/°C
Efficiency(/ Module area)	Eff_mod	16,5	%	Fill factor	FF	0,773	
Efficiency(/ Cells area)	Eff_cells	18,3	%				

PV module: Axitec Energy, AXIpower AC-320P/72S

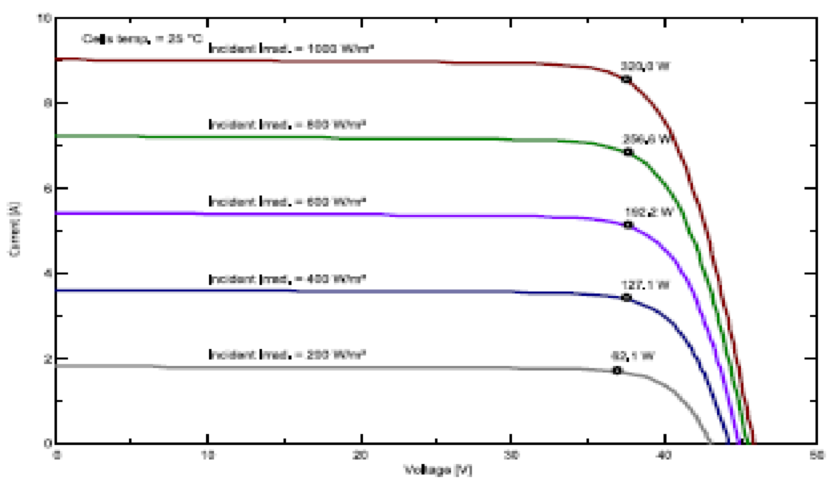

Appendix C: Maslmani PV-syst analysis

PVSYST V6.78		04/02/19	Page 1/1

Characteristics of a PV module

Manufacturer, model :	**Axitec Energy, AXIpower AC-320P/72S**
Availability :	Prod. Since 2015
Data source :	Manufacturer 2018

STC power (manufacturer)	**Pnom**	**320**	**Wp**	**Technology**		**Si-poly**	
Module size (W x L)		0.992 x 1.956	m²	Rough module area	Amodule	1.94	m²
Number of cells		1 x 72		Sensitive area (cells)	Acells	1.75	m²
Specifications for the model (manufacturer or measurement data)							
Reference temperature	TRef	25	°C	Reference irradiance	GRef	1000	W/m²
Open circuit voltage	Voc	45.8	V	Short-circuit current	Isc	9.03	A
Max. power point voltage	Vmpp	37.6	V	Max. power point current	Impp	8.52	A
=> maximum power	Pmpp	320.0	W	Isc temperature coefficient	muIsc	3.6	mA/°C
One-diode model parameters							
Shunt resistance	Rshunt	350	ohm	Diode saturation current	IoRef	0.028	nA
Serie resistance	Rserie	0.34	ohm	Voc temp. coefficient	MuVoc	-149	mV/°C
				Diode quality factor	Gamma	0.94	
Specified Pmax temper. coeff.	muPMaxR	-0.40	%/°C	Diode factor temper. coeff.	muGamma	0.000	1/°C
Reverse Bias Parameters, for use in behaviour of PV arrays under partial shadings or mismatch							
Reverse characteristics (dark)	BRev	3.20	mA/V²	(quadratic factor (per cell))			
Number of by-pass diodes per module		3		Direct voltage of by-pass diodes		-0.7	V
Model results for standard conditions (STC: T=25°C, G=1000 W/m², AM=1,5)							
Max. power point voltage	Vmpp	37.5	V	Max. power point current	Impp	8.52	A
Maximum power	Pmpp	320.0	Wc	Power temper. coefficient	muPmpp	-0.39	%/°C
Efficiency(/ Module area)	Eff_mod	16.5	%	Fill factor	FF	0.773	
Efficiency(/ Cells area)	Eff_cells	18.3	%				

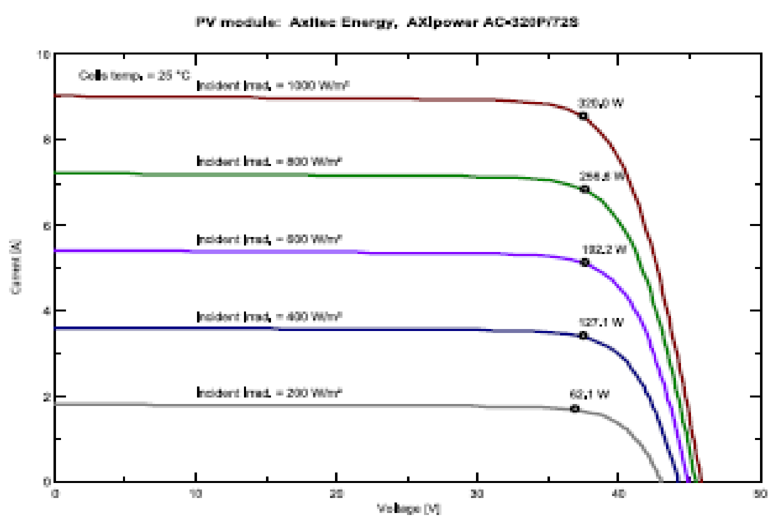

Characteristics of a grid inverter

Manufacturer, model :	**SMA, Sunny Tripower 60-10**
Availability :	Prod. Since 2015
Data source :	Manufacturer 2015

570

Operating mode		**MPPT**			
Minimum MPP Voltage	**Vmin**	**N/A V**	Nominal PV Power	Pnom DC	61 kW
Maximum MPP Voltage	**Vmax**	**800 V**	Maximum PV Power	Pmax DC	61 kW
Absolute max. PV Voltage	Vmax array	1000 V	Maximum PV Current	Imax DC	N/A A
Min. Voltage for PNom	Vmin PNom	N/A V	Power Threshold	Pthresh.	100 W
Behaviour at Vmin/Vmax		Limitation	Behaviour at Pnom		Limitation

Output characteristics (AC grid side)

Grid Voltage	Unom	400 V	**Nominal AC Power**	**Pnom AC**	**60 kWac**
Grid frequency	Freq	50 Hz	Maximum AC Power	Pmax AC	60 kWac
	Triphased		Nominal AC current	Inom AC	87 A
			Maximum AC current	Imax AC	87 A

Efficiency defined for 3 voltages	570 V	630 V	800 V
Maximum efficiency	98.8 %	98.5 %	98.1 %
European average efficiency	98.5 %	98.3 %	97.8 %

Remarks and Technical features

Array isolation monitoring, Internal DC switch,
Output Voltage disconnect adjustement, ENS protection,

Technology: TL
Protection: -25 - +60°C, IP 65: outdoor installation
Control: Graphic
Separate string combiner required!

Sizes:	
Width	570 mm
Height	740 mm
Depth	300 mm
Weight	75.00 kg

Efficiency profile vs Output power

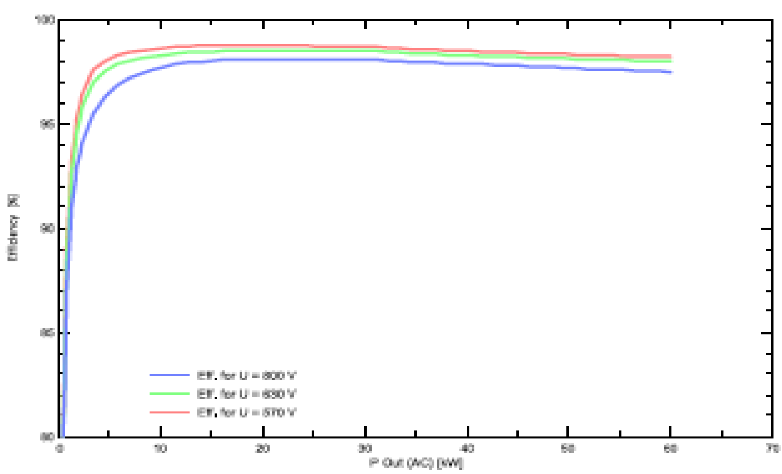

PVSYST V6.78		04/02/19	Page 1/3

Grid-Connected System: Simulation parameters

Project : Maslamani 1887 kWp

Geographical Site	**Tubas**		Country	Palestine
Situation	Latitude	N 32.19	Longitude	35.22° E
Time defined as	Legal Time	Time zone UT+2	Altitude	320m
	Albedo	0.20		
Meteo data:	**Jerusalem**	Synthetic		

Simulation variant : New simulation variant320

Simulation date 04/02/19 22h25

Simulation parameters	System type	**No 3D scene defined, no shadings**		
Collector Plane Orientation	Tilt	28°	Azimuth	0°
Models used	Transposition	Perez	Diffuse	Perez, Meteonorm
Horizon	Free Horizon			
Near Shadings	No Shadings			
User's needs :	Unlimited load (grid)			

PV Array Characteristics

PV module	Si-poly	Model	**AXIpower AC-320P/72S**		
Original PVsyst database		Manufacturer	Axitec Energy		
Number of PV modules		In series	19 modules	In parallel	310 strings
Total number of PV modules		Nb. modules	5890	Unit Nom. Power	320 Wp
Array global power		Nominal (STC)	**1885 kWp**	At operating cond.	1696 kWp (50°C)
Array operating characteristics (50°C)		U mpp	641 V	I mpp	2646 A
Total area		Module area	**11429 m²**	Cell area	10320 m²

Inverter	Model	**Sunny Tripower 60-10**		
Original PVsyst database	Manufacturer	SMA		
Characteristics	Operating Voltage	570-800 V	Unit Nom. Power	60,0 kWac
Inverter pack	Nb. of inverters	26 units	Total Power	1560 kWac
			Pnom ratio	1.21

PV Array loss factors

Array Soiling Losses			Loss Fraction	3.0 %
Thermal Loss factor	Uc (const)	20.0 W/m²K	Uv (wind)	0.0 W/m²K / m/s
Wiring Ohmic Loss	Global array res.	4,1 mOhm	Loss Fraction	1,5 % at STC
Module Quality Loss			Loss Fraction	-0,4 %
Module Mismatch Losses			Loss Fraction	1.0 % at MPP

Incidence effect (IAM): Fresnel smooth glass, n = 1.526

0°	30°	50°	60°	70°	75°	80°	85°	90°
1.000	0.998	0.981	0.948	0.862	0.776	0.636	0.403	0.000

PVSYST V6.78		04/02/19	Page 1/1

Definition of a geographical site

Geographical Site **Tubas** Country **Israel**

File Tubas_MN71mod.SIT of 04/02/19 21h57

Situation Latitude 32.19° N Longitude 35.29° E
Time defined as Legal Time Time zone UT+2 Altitude 320 m

Monthly Meteo Values Source MeteoNorm 7.1 station (modified by user)

	Jan.	Feb.	Mar.	Apr.	May	June	July	Aug.	Sep.	Oct.	Nov.	Dec.	Year	
Hor. global	88.1	100.8	159.0	187.1	229.8	245.0	247.9	228.1	184.2	142.9	103.9	85.7	2002.5	kWh/m².mth
Hor. diffuse	41.9	43.3	58.9	64.5	61.9	54.4	56.4	53.6	50.0	43.6	34.0	35.8	598.3	kWh/m².mth
Extraterrestrial	175.3	197.3	267.3	304.8	344.5	344.2	350.4	327.2	277.0	235.5	181.0	162.6	3167.2	kWh/m².mth
Clearness Index	0.502	0.511	0.595	0.614	0.667	0.712	0.708	0.697	0.665	0.607	0.574	0.527	0.632	
Amb. temper.	7.5	8.8	12.6	16.4	20.9	24.0	26.1	25.6	23.0	20.0	13.6	9.4	17.3	°C
Wind velocity	3.0	3.4	3.1	3.3	3.3	3.3	3.6	3.1	2.6	2.1	2.3	2.7	3.0	m/s

Solar paths at Tubas, (Lat. 32.1900° N, long. 35.2900° E, alt. 320 m) - Legal Time

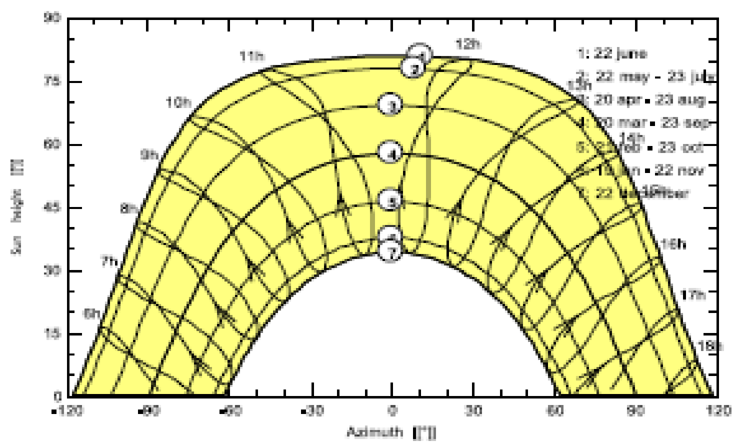

PVSYST V6.78		04/02/19	Page 1/3

Grid-Connected System: Simulation parameters

Project : Maslamani 1121 kWp

Geographical Site	**Tubas**		Country	**Palestine**
Situation	Latitude	32.19 N	Longitude	35.29
Time defined as	Legal Time	Time zone UT+2	Altitude	320m
	Albedo	0.20		
Meteo data:	**Jerusalem**	Synthetic		

Simulation variant : New simulation variant320

Simulation date 04/02/19 22h53

Simulation parameters	System type	**No 3D scene defined, no shadings**		
Collector Plane Orientation	Tilt	28°	Azimuth	0°
Models used	Transposition	Perez	Diffuse	Perez, Meteonorm
Horizon	Free Horizon			
Near Shadings	No Shadings			
User's needs :	Unlimited load (grid)			

PV Array Characteristics

PV module	Si-poly	Model	**AXIpower AC-320P/72S**		
Original PVsyst database		Manufacturer	Axitec Energy		
Number of PV modules		In series	19 modules	In parallel	184 strings
Total number of PV modules		Nb. modules	3496	Unit Nom. Power	320 Wp
Array global power		Nominal (STC)	**1119 kWp**	At operating cond.	1007 kWp (50°C)
Array operating characteristics (50°C)		U mpp	641 V	I mpp	1570 A
Total area		Module area	**6783 m²**	Cell area	6126 m²
Inverter		Model	**Sunny Tripower 60-10**		
Original PVsyst database		Manufacturer	SMA		
Characteristics		Operating Voltage	570-800 V	Unit Nom. Power	60.0 kWac
Inverter pack		Nb. of inverters	15 units	Total Power	900 kWac
				Pnom ratio	1.24

PV Array loss factors

Array Soiling Losses			Loss Fraction	3.0 %
Thermal Loss factor	Uc (const)	20.0 W/m²K	Uv (wind)	0.0 W/m²K / m/s
Wiring Ohmic Loss	Global array res.	6.8 mOhm	Loss Fraction	1.5 % at STC
Module Quality Loss			Loss Fraction	-0.4 %
Module Mismatch Losses			Loss Fraction	1.0 % at MPP

Incidence effect (IAM): Fresnel smooth glass, n = 1.526

0°	30°	50°	60°	70°	75°	80°	85°	90°
1.000	0.998	0.981	0.948	0.862	0.776	0.636	0.403	0.000

Appendix D: Czechia PV-syst analysis

PVSYST V6,78		04/02/19	Page 1/1

Characteristics of a grid inverter

Manufacturer, model :	**ABB, TRIO-27.6-TL-OUTD-400 (27.6 kWac max)**
Availability :	Prod. Since 2011
Data source :	Manufacturer 2017

200

Operating mode		**MPPT**			
Minimum MPP Voltage	**Vmin**	**N/A V**	Nominal PV Power	Pnom DC	29 kW
Maximum MPP Voltage	**Vmax**	**950 V**	Maximum PV Power	Pmax DC	29 kW
Absolute max. PV Voltage	Vmax array	1000 V	Maximum PV Current	Imax DC	N/A A
Min. Voltage for PNom	Vmin PNom	500 V	Power Threshold	Pthresh.	140 W
Multi MPPT capability			Number of MPPT inputs		2
Behaviour at Vmin/Vmax		Limitation	Behaviour at Pnom		Limitation

Output characteristics (AC grid side)

Grid Voltage	Unom	400 V	**Nominal AC Power**	**Pnom AC**	**28 kWac**
Grid frequency	Freq	50 Hz	Maximum AC Power	Pmax AC	28 kWac
	Triphased		Nominal AC current	Inom AC	45 A
			Maximum AC current	Imax AC	45 A

Efficiency defined for 3 voltages	500 V	620 V	800 V
Maximum efficiency	97.5 %	98.2 %	97.7 %
European average efficiency	97.1 %	97.9 %	97.3 %

Remarks and Technical features

Array isolation monitoring, Internal DC switch,
Internal AC switch, ENS protection,

Technology: Dual stage transformerless topology PV inverter.
Protection:
Control:

Sizes:		
	Width	702 mm
	Height	1061 mm
	Depth	292 mm
	Weight	75.00 kg

Efficiency profile vs Output power

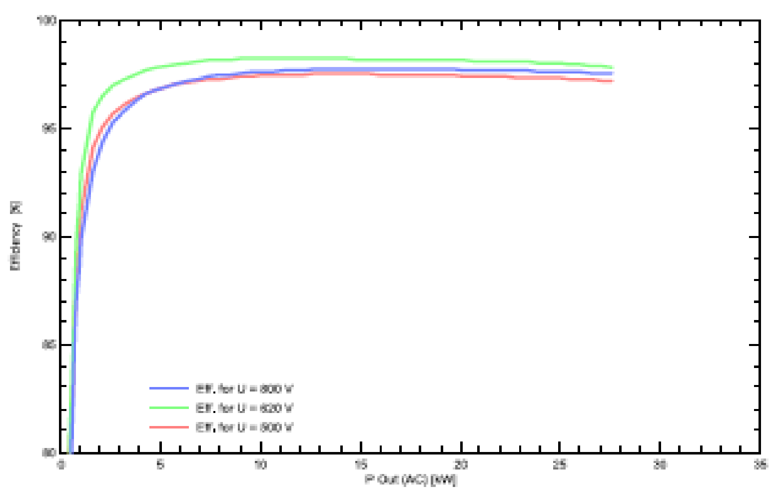

PVSYST V6.78		04/02/19	Page 1/1

Characteristics of a PV module

Manufacturer, model : **Hanwha Q Cells, Q.PRO-G2 250**

Availability : Prod. from 2012 to 2013

Data source : Manufacturer 2013

STC power (manufacturer)	**Pnom**	**250**	**Wp**	**Technology**		**Si-poly**	
Module size (W x L)		1,000 x 1,670	m²	Rough module area	Amodule	1,67	m²
Number of cells		1 x 60		Sensitive area (cells)	Acells	1,46	m²

Specifications for the model (manufacturer or measurement data)

Reference temperature	TRef	25	°C	Reference irradiance	GRef	1000	W/m²
Open circuit voltage	Voc	37.8	V	Short-circuit current	Isc	8.94	A
Max. power point voltage	Vmpp	29.9	V	Max. power point current	Impp	8.36	A
=> maximum power	Pmpp	250.0	W	Isc temperature coefficient	muIsc	3.6	mA/°C

One-diode model parameters

Shunt resistance	Rshunt	300	ohm	Diode saturation current	IoRef	2.17	nA
Serie resistance	Rserie	0.35	ohm	Voc temp. coefficient	MuVoc	-126	mV/°C
				Diode quality factor	Gamma	1.11	
Specified Pmax temper. coeff.	muPMaxR	-0.43	%/°C	Diode factor temper. coeff.	muGamma	0.000	1/°C

Reverse Bias Parameters, for use in behaviour of PV arrays under partial shadings or mismatch

Reverse characteristics (dark)	BRev	3.20	mA/V²	(quadratic factor (per cell))	
Number of by-pass diodes per module		3		Direct voltage of by-pass diodes	-0.7 V

Model results for standard conditions (STC: T=25°C, G=1000 W/m², AM=1.5)

Max. power point voltage	Vmpp	30.0	V	Max. power point current	Impp	8.34	A
Maximum power	Pmpp	250.0	Wc	Power temper. coefficient	muPmpp	-0.43	%/°C
Efficiency(/ Module area)	Eff_mod	15.0	%	Fill factor	FF	0.740	
Efficiency(/ Cells area)	Eff_cells	17.1	%				

PV module: Hanwha Q Cells, Q.PRO-G2 250

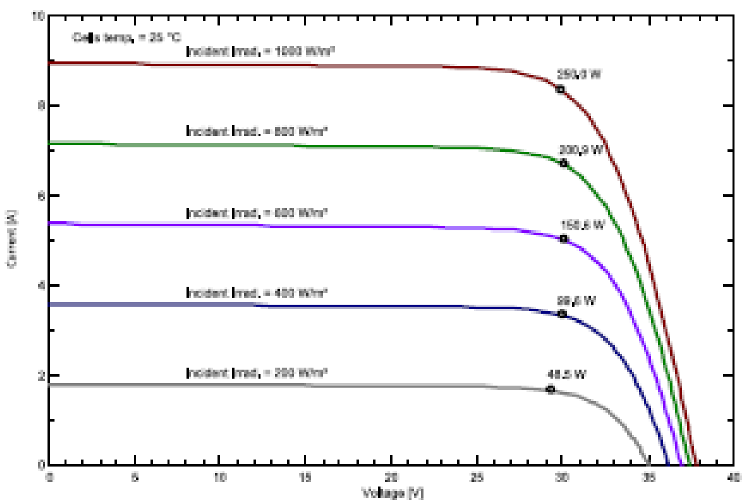

Grid-Connected System: Simulation parameters

Project : Czechia 350 kWp

Geographical Site	Tubas		Country	Palestine
Situation	Latitude	32.19 N	Longitude	35.29 E
Time defined as	Legal Time	Time zone UT+2	Altitude	802 m
	Albedo	0.20		
Meteo data:	**Jerusalem**	Synthetic		

Simulation variant : **New simulation variant320**

Simulation date 04/02/19 23h16

Simulation parameters	System type	**No 3D scene defined, no shadings**		
Collector Plane Orientation	Tilt	28°	Azimuth	0°
Models used	Transposition	Perez	Diffuse	Perez, Meteonorm
Horizon	Free Horizon			
Near Shadings	No Shadings			
User's needs :	Unlimited load (grid)			

PV Array Characteristics

PV module	Si-poly	Model	**Q.PRO-G2 250**		
Original PVsyst database		Manufacturer	Hanwha Q Cells		
Number of PV modules		In series	20 modules	In parallel	70 strings
Total number of PV modules		Nb. modules	1400	Unit Nom. Power	250 Wp
Array global power		Nominal (STC)	**350 kWp**	At operating cond.	312 kWp (50°C)
Array operating characteristics (50°C)		U mpp	536 V	I mpp	583 A
Total area		Module area	**2338 m²**	Cell area	2045 m²
Inverter		Model	**TRIO-27,6-TL-OUTD-400 (27,6 kWac max)**		
Original PVsyst database		Manufacturer	ABB		
Characteristics		Operating Voltage	200-950 V	Unit Nom. Power	27,6 kWac
Inverter pack		Nb. of inverters	20 * MPPT 50 %	Total Power	276 kWac
				Pnom ratio	1,27

PV Array loss factors

Array Soiling Losses			Loss Fraction	3.0 %
Thermal Loss factor	Uc (const)	20.0 W/m²K	Uv (wind)	0.0 W/m²K / m/s
Wiring Ohmic Loss	Global array res.	15 mOhm	Loss Fraction	1,5 % at STC
Module Quality Loss			Loss Fraction	-0,5 %
Module Mismatch Losses			Loss Fraction	1.0 % at MPP
Incidence effect, ASHRAE parametrization	IAM =	1 - bo (1/cos i - 1)	bo Param.	0.05

PVSYST V6.78		04/02/19	Page 1/3

Grid-Connected System: Simulation parameters

Project : **Czechia 120 kWp**

Geographical Site	**Tubas**		Country	Palestine
Situation	Latitude	32.19 N	Longitude	35.29E
Time defined as	Legal Time	Time zone UT+2	Altitude	320m
	Albedo	0.20		
Meteo data:	**Jerusalem**	Synthetic		

Simulation variant : **New simulation variant320**

Simulation date 04/02/19 23h29

Simulation parameters	System type	**No 3D scene defined, no shadings**		
Collector Plane Orientation	Tilt	28°	Azimuth	0°
Models used	Transposition	Perez	Diffuse	Perez, Meteonorm
Horizon	Free Horizon			
Near Shadings	No Shadings			
User's needs :	Unlimited load (grid)			

PV Array Characteristics

PV module Si-poly	Model	**Q.PRO-G2 250**		
Original PVsyst database	Manufacturer	Hanwha Q Cells		
Number of PV modules	In series	20 modules	In parallel	24 strings
Total number of PV modules	Nb. modules	480	Unit Nom. Power	250 Wp
Array global power	Nominal (STC)	**120 kWp**	At operating cond.	107 kWp (50°C)
Array operating characteristics (50°C)	U mpp	536 V	I mpp	200 A
Total area	Module area	**802 m²**	Cell area	701 m²
Inverter	Model	**TRIO-27.6-TL-OUTD-400 (27.6 kWac max)**		
Original PVsyst database	Manufacturer	ABB		
Characteristics	Operating Voltage	200-950 V	Unit Nom. Power	27.6 kWac
Inverter pack	Nb. of inverters	7 * MPPT 50 %	Total Power	97 kWac
			Pnom ratio	1.24

PV Array loss factors

Array Soiling Losses			Loss Fraction	3.0 %
Thermal Loss factor	Uc (const)	20.0 W/m²K	Uv (wind)	0.0 W/m²K / m/s
Wiring Ohmic Loss	Global array res.	45 mOhm	Loss Fraction	1.5 % at STC
Module Quality Loss			Loss Fraction	-0.5 %
Module Mismatch Losses			Loss Fraction	1.0 % at MPP
Incidence effect, ASHRAE parametrization	IAM =	1 - bo (1/cos i - 1)	bo Param.	0.05

Appendix F1: All data of the distribution line

Project:		ETAP	Page:	1
Location:		16.0.0C	Date:	17-03-2019
Contract:			SN:	4359168
Engineer:		Study Case: LF	Revision:	Base
Filename:	tobas2		Config.:	Normal

Line/Cable Input Data

ohms or siemens/1000 m per Conductor (Cable) or per Phase (Line)

Line/Cable ID	Library	Size	Length Adj. (m)	Length % Tol.	#/Phase	T (°C)	R	X	Y
Line1		120	955.0	0.0	1	75	0.413000	0.352573	0.0000034
Line2		182	1000.0	0.0	1	75	0.249000	0.324378	0.0000036
Line3		182	316.0	0.0	1	75	0.249000	0.324378	0.0000036
line3		182	1404.0	0.0	1	75	0.249000	0.324378	0.0000036
Line4		182	1000.0	0.0	1	75	0.249000	0.324378	0.0000036
Line5		182	369.0	0.0	1	75	0.249000	0.324378	0.0000036
Line6		182	227.0	0.0	1	75	0.249000	0.324378	0.0000036
Line7		182	110.0	0.0	1	75	0.249000	0.324378	0.0000036
Line8		182	440.0	0.0	1	75	0.249000	0.324378	0.0000036
Line9		182	750.0	0.0	1	75	0.249000	0.324378	0.0000036
Line10		182	224.0	0.0	1	75	0.249000	0.324378	0.0000036
Line11		182	189.0	0.0	1	75	0.249000	0.324378	0.0000036
Line12		182	525.0	0.0	1	75	0.249000	0.324378	0.0000036
Line13		182	325.0	0.0	1	75	0.249000	0.324378	0.0000036
Line14		182	133.0	0.0	1	75	0.249000	0.324378	0.0000036
Line15		182	420.0	0.0	1	75	0.249000	0.324378	0.0000036
Line16		182	1429.0	0.0	1	75	0.249000	0.324378	0.0000036
Line17		182	425.0	0.0	1	75	0.249000	0.324378	0.0000036
Line18		182	644.0	0.0	1	75	0.249000	0.324378	0.0000036
Line19		182	305.0	0.0	1	75	0.249000	0.324378	0.0000036
Line20		182	1000.0	0.0	1	75	0.249000	0.324378	0.0000036
Line21		182	279.0	0.0	1	75	0.249000	0.324378	0.0000036
Line22		182	133.0	0.0	1	75	0.249000	0.324378	0.0000036
Line23		182	1349.0	0.0	1	75	0.249000	0.324378	0.0000036
Line24		182	1632.0	0.0	1	75	0.249000	0.324378	0.0000036
Line25		182	200.0	0.0	1	75	0.249000	0.324378	0.0000036

Line / Cable resistances are listed at the specified temperatures.

Appendix F2: Data of the transformer

Project:	ETAP	Page: 1
Location:	16.0.0C	Date: 17-03-2019
Contract:		SN: 4359168
Engineer:	Study Case: LF	Revision: Base
Filename: tobas2		Config.: Normal

2-Winding Transformer Input Data

Transformer		Rating					Z Variation			% Tap Setting		Adjusted	Phase Shift	
ID	Phase	MVA	Prim. kV	Sec. kV	% Z1	X1/R1	+ 5%	- 5%	% Tol.	Prim.	Sec.	% Z	Type	Angle
T1	3-Phase	0.160	33.000	0.400	4.00	1.50	0	0	0	0	0	4.0000	Dyn	0.000
T3	3-Phase	0.250	33.000	0.400	4.00	1.50	0	0	0	0	0	4.0000	Dyn	0.000
T4	3-Phase	0.160	33.000	0.400	4.00	1.50	0	0	0	0	0	4.0000	Dyn	0.000
T6	3-Phase	0.160	33.000	0.400	4.00	1.50	0	0	0	0	0	4.0000	Dyn	0.000
T8	3-Phase	0.400	33.000	0.400	4.00	1.50	0	0	0	0	0	4.0000	Dyn	0.000
T10	3-Phase	0.160	33.000	0.400	4.00	1.50	0	0	0	0	0	4.0000	Dyn	0.000
T12	3-Phase	0.250	33.000	0.400	4.00	1.50	0	0	0	0	0	4.0000	Dyn	0.000
T14	3-Phase	0.250	33.000	0.400	4.00	1.50	0	0	0	0	0	4.0000	Dyn	0.000
T16	3-Phase	0.400	33.000	0.400	4.00	1.50	0	0	0	0	0	4.0000	Dyn	0.000
T18	3-Phase	0.630	33.000	0.400	4.00	1.50	0	0	0	0	0	4.0000	Dyn	0.000
T20	3-Phase	30.000	33.000	0.400	4.00	1.50	0	0	0	0	0	4.0000	Dyn	0.000
T22	3-Phase	0.400	33.000	0.400	4.00	1.50	0	0	0	0	0	4.0000	Dyn	0.000
T24	3-Phase	3.000	33.000	0.400	6.25	6.00	0	0	0	0	0	6.2500	Dyn	0.000
T26	3-Phase	0.160	33.000	0.400	4.00	1.50	0	0	0	0	0	4.0000	Dyn	0.000
T28	3-Phase	0.400	33.000	0.400	4.00	1.50	0	0	0	0	0	4.0000	Dyn	0.000
T30	3-Phase	0.050	33.000	0.400	4.00	1.50	0	0	0	0	0	4.0000	Dyn	0.000
T30	3-Phase	0.050	33.000	0.400	4.00	1.50	0	0	0	0	0	4.0000	Dyn	0.000
T32	3-Phase	0.400	33.000	0.400	4.00	1.50	0	0	0	0	0	4.0000	Dyn	0.000
T34	3-Phase	0.400	33.000	0.400	4.00	1.50	0	0	0	0	0	4.0000	Dyn	0.000
T36	3-Phase	0.400	33.000	0.400	6.25	6.00	0	0	0	0	0	6.2500	Dyn	0.000
T38	3-Phase	5.000	33.000	0.400	6.25	6.00	0	0	0	0	0	6.2500	Dyn	0.000
T40	3-Phase	0.250	33.000	0.400	4.00	1.50	0	0	0	0	0	4.0000	Dyn	0.000
T42	3-Phase	0.250	33.000	0.400	4.00	1.50	0	0	0	0	0	4.0000	Dyn	0.000
T44	3-Phase	0.400	33.000	0.400	4.00	1.50	0	0	0	0	0	4.0000	Dyn	0.000
T46	3-Phase	3.000	33.000	0.400	6.25	6.00	0	0	0	0	0	6.2500	Dyn	0.000
T47	3-Phase	3.000	33.000	0.400	6.25	6.00	0	0	0	0	0	6.2500	Dyn	0.000

Appendix F3: Output result from the ETAP

Project:		ETAP	Page:	1
Location:		16.0.0C	Date:	17-03-2019
Contract:			SN:	4359168
Engineer:		Study Case: LF	Revision:	Base
Filename:	tobas2		Config.:	Normal

LOAD FLOW REPORT

Bus		Voltage		Generation		Load		Load Flow					XFMR
ID	kV	% Mag.	Ang.	MW	Mvar	MW	Mvar	ID	MW	Mvar	Amp	%PF	%Tap
* Bus1	33.000	100.000	0.0	14.003	6.138	0	0	Bus2	0.042	0.009	0.8	97.8	
								Bus5	13.961	6.129	266.8	91.6	
Bus2	33.000	99.998	0.0	0	0	0	0	Bus1	-0.042	-0.013	0.8	95.8	
								Bus53	0.042	0.013	0.8	95.8	
Bus5	33.000	99.499	-0.2	0	0	0	0	Bus1	-13.908	-6.063	266.8	91.7	
								Bus7	13.889	6.057	266.4	91.7	
								Bus6	0.019	0.006	0.3	94.9	
Bus6	0.400	99.248	-0.3	0	0	0.019	0.006	Bus5	-0.019	-0.006	28.7	95.0	
Bus7	33.000	98.797	-0.4	0	0	0	0	Bus9	13.796	5.959	266.1	91.8	
								Bus5	-13.815	-5.965	266.5	91.8	
Bus2	33.000	99.998	0.0	0	0	0	0	Bus1	-0.042	-0.013	0.8	95.8	
								Bus53	0.042	0.013	0.8	95.8	
Bus5	33.000	99.499	-0.2	0	0	0	0	Bus1	-13.908	-6.063	266.8	91.7	
								Bus7	13.889	6.057	266.4	91.7	
								Bus6	0.019	0.006	0.3	94.9	
Bus6	0.400	99.248	-0.3	0	0	0.019	0.006	Bus5	-0.019	-0.006	28.7	95.0	
Bus7	33.000	98.797	-0.4	0	0	0	0	Bus9	13.796	5.959	266.1	91.8	
								Bus5	-13.815	-5.965	266.5	91.8	
								Bus8	0.019	0.006	0.3	94.9	
Bus8	0.400	98.406	-0.6	0	0	0.019	0.006	Bus7	-0.019	-0.006	28.6	95.0	
Bus9	33.000	98.639	-0.4	0	0	0	0	Bus7	-13.779	-5.939	266.1	91.8	
								Bus11	13.662	5.907	264.0	91.8	
								Bus10	0.117	0.032	2.2	96.5	
Bus10	0.400	96.337	-1.6	0	0	0.115	0.029	Bus9	-0.115	-0.029	177.9	97.0	
Bus11	33.000	98.144	-0.6	0	0	0	0	Bus9	-13.610	-5.842	264.0	91.9	
								Bus13	13.486	5.810	261.8	91.8	
								Bus12	0.124	0.032	2.3	96.8	
Bus12	0.400	97.176	-1.1	0	0	0.123	0.031	Bus11	-0.123	-0.031	188.0	97.0	
Bus13	33.000	97.963	-0.7	0	0	0	0	Bus11	-13.467	-5.787	261.8	91.9	
								Bus15	13.536	5.704	262.3	92.2	
								Bus46	-0.069	0.083	1.9	-63.9	
Bus14	0.400	97.074	-1.0	0	0	0.036	0.012	Bus15	-0.036	-0.012	57.0	95.0	
Bus15	33.000	97.852	-0.7	0	0	0	0	Bus13	-13.524	-5.690	262.3	92.2	
								Bus16	13.488	5.678	261.6	92.2	
								Bus14	0.037	0.012	0.7	94.8	

Activate Windows
Go to Settings to activate Windows.

Bus		Voltage		Generation		Load		Load Flow					XFMR
ID	kV	% Mag.	Ang.	MW	Mvar	MW	Mvar	ID	MW	Mvar	Amp	%PF	%Tap
Bus19	0.400	97.485	-0.8	0	0	0	0	Bus18	0.000	0.000	0.1	100.0	
Bus20	33.000	97.583	-0.8	0	0	0	0	Bus17	-0.168	-0.059	3.2	94.4	
								Bus22	0.168	0.059	3.2	94.4	
Bus21	0.400	98.065	-0.3	0.244	0.000	0	0	Bus52	0.244	0.000	359.3	100.0	
Bus22	0.400	95.274	-1.8	0	0	0.165	0.054	Bus20	-0.165	-0.054	262.8	95.0	
Bus23	33.000	97.461	-0.8	0	0	0	0	Bus18	-2.893	-2.059	63.7	81.5	
								Bus26	2.674	1.991	59.8	80.2	
								Bus25	0.219	0.068	4.1	95.6	
Bus24	0.400	98.011	-0.5	0.086	0.000	0	0	Bus52	0.086	0.000	126.5	100.0	
Bus25	0.400	95.648	-1.7	0	0	0.216	0.063	Bus23	-0.216	-0.063	339.7	96.0	
Bus26	33.000	97.396	-0.8	0	0	0	0	Bus23	-2.673	-1.991	59.9	80.2	
								Bus27	2.430	1.939	55.8	78.2	
								Bus28	0.242	0.052	4.5	97.8	
Bus27	33.000	97.358	-0.8	0	0	0	0	Bus26	-2.429	-1.939	55.9	78.2	
Bus26	33.000	97.396	-0.8	0	0	0	0	Bus23	-2.673	-1.991	59.9	80.2	
								Bus27	2.430	1.939	55.8	78.2	
								Bus28	0.242	0.052	4.5	97.8	
Bus27	33.000	97.358	-0.8	0	0	0	0	Bus26	-2.429	-1.939	55.9	78.2	
								Bus30	0.212	0.145	4.6	82.5	
								Bus33	0.338	1.094	20.6	29.5	
								Bus32	1.880	0.700	36.0	93.7	
Bus28	0.400	96.243	-1.5	0	0	0.240	0.049	Bus26	-0.240	-0.049	367.5	98.0	
Bus29	0.400	96.399	-1.3	0	0	10.302	3.386	Bus17	-10.302	-3.386	16237.2	95.0	
Bus30	33.000	97.357	-0.8	0	0	0	0	Bus27	-0.212	-0.145	4.6	82.4	
								Bus31	0.212	0.145	4.6	82.4	
Bus31	0.400	94.915	-1.4	0	0	0.208	0.140	Bus30	-0.208	-0.140	380.5	83.0	
Bus32	0.400	95.292	-3.1	0	0	1.865	0.613	Bus27	-1.865	-0.613	2973.7	95.0	
Bus33	33.000	97.341	-0.8	0	0	0	0	Bus27	-0.338	-1.095	20.6	29.5	
								Bus35	0.292	1.082	20.1	26.1	
								Bus34	0.046	0.014	0.9	95.8	
Bus34	0.400	96.401	-1.3	0	0	0.045	0.013	Bus33	-0.045	-0.013	70.7	96.0	
Bus35	33.000	97.284	-0.8	0	0	0	0	Bus33	-0.292	-1.086	20.2	26.0	
								Bus37	0.203	1.042	19.1	19.1	
								Bus36	0.089	0.044	1.8	89.8	
Bus36	0.400	96.400	-1.1	0	0	0.089	0.043	Bus35	-0.089	-0.043	147.7	90.0	
Bus37	33.000	97.268	-0.8	0	0	0	0	Bus35	-0.203	-1.044	19.1	19.0	
								Bus39	0.185	1.036	18.9	17.6	
								Bus38	0.017	0.008	0.3	90.6	
Bus38	0.400	95.937	-1.3	0	0	0.017	0.008	Bus37	-0.017	-0.008	28.2	91.0	
Bus39	33.000	97.245	-0.8	0	0	0	0	Bus37	-0.185	-1.038	19.0	17.6	

Bus41	33.000	97.254	-0.8	0	0	0	0	Bus39	1.723	-0.383	31.7	-97.6
								Bus40	0.171	0.058	3.2	94.6
								Bus54	-1.893	0.325	34.6	-98.6
Bus42	33.000	97.180	-0.8	0	0	0	0	Bus39	-1.907	-0.658	36.3	94.5
								Bus44	1.791	0.632	34.2	94.3
								Bus43	0.116	0.026	2.1	97.6
Bus43	0.400	96.479	-1.9	0	0	0.116	0.024	Bus42	-0.116	-0.024	176.8	98.0
Bus44	33.000	97.163	-0.8	0	0	0	0	Bus42	-1.790	-0.633	34.2	94.3
								Bus45	1.790	0.633	34.2	94.3
Bus45	0.400	96.005	-2.1	0	0	1.782	0.586	Bus44	-1.782	-0.586	2820.9	95.0
Bus46	33.000	97.963	-0.7	0	0	0	0	Bus13	0.069	-0.083	1.9	-63.6
								Bus47	-0.189	0.034	3.4	-98.5
								Bus48	0.121	0.049	2.3	92.5
Bus47	33.000	97.968	-0.6	0	0	0	0	Bus46	0.189	-0.039	3.4	-98.0
								Bus50	-0.314	0.000	5.6	100.0
								Bus49	0.125	0.038	2.3	95.6
Bus48	0.400	96.205	-1.4	0	0	0.119	0.047	Bus46	-0.119	-0.047	192.1	93.0
Bus49	0.400	96.329	-1.5	0	0	0.123	0.036	Bus47	-0.123	-0.036	192.0	96.0
Bus50	33.000	97.979	-0.6	0	0	0	0	Bus47	0.314	-0.006	5.6	-100.0
								Bus52	-0.330	0.001	5.9	100.0
								Bus51	0.016	0.006	0.3	94.0
Bus51	0.400	97.841	-0.7	0	0	0.016	0.006	Bus50	-0.016	-0.006	24.9	94.0
Bus52	33.000	97.981	-0.6	0	0	0	0	Bus50	0.330	-0.001	5.9	100.0
								Bus21	-0.244	0.001	4.4	100.0
								Bus24	-0.086	0.000	1.5	100.0
Bus53	0.400	99.158	-0.4	0	0	0.042	0.012	Bus2	-0.042	-0.012	63.2	96.0
Bus54	0.400	106.812	9.0	2.110	0.000	0	0	Bus41	2.110	0.000	2851.2	100.0